Defense Threat Reduction Agency
8725 John J. Kingman Road, MS
6201 Fort Belvoir, VA 22060-6201

DTRA-TR-13-48

TECHNICAL REPORT

Low Power, Room Temperature Systems for the Detection and Identification of Radionuclides from Atmospheric Nuclear Test

Approved for public release; distribution is unlimited.

July 2013

DTRA01-01-C-0071

Muren Chu, et al.

Prepared by:
Fermionics Corporation
4555 Runway St
Simmi Valley, CA 93063

DTRA 13 048

DESTRUCTION NOTICE:

REPORT DOCUMENTATION PAGE

Form Approved
OMB No. 0704-0188

1. REPORT DATE (DD-MM-YYYY)	2. REPORT TYPE	3. DATES COVERED (From - To)
00-07-2013	Technical	Sept. 1, 2001 - February 29, 2004

4. TITLE AND SUBTITLE

Low Power, Room Temperature Systems for the Detection and Identification of Radionuclides from Atmospheric Nuclear Tests

5a. CONTRACT NUMBER
DTRA01-01-C-0071

5b. GRANT NUMBER

5c. PROGRAM ELEMENT NUMBER

6. AUTHOR(S)

Muren Chu, Sevag Terterian, and David Ting

5d. PROJECT NUMBER

5e. TASK NUMBER

5f. WORK UNIT NUMBER

7. PERFORMING ORGANIZATION NAME(S) AND ADDRESS(ES)

Ferionics Corporation
4555 Runway St.
Simi Valley, CA 93063

8. PERFORMING ORGANIZATION REPORT NUMBER

2450-04F

9. SPONSORING / MONITORING AGENCY NAME(S) AND ADDRESS(ES)

Defense Threat Reduction Agency
8725 John J. Kingman Road, STOP 6201
Fort Belvoir, VA 22060
PM/LTC T. Cartledge

10. SPONSOR/MONITOR'S ACRONYM(S)

DTRA

11. SPONSOR/MONITOR'S REPORT NUMBER(S)

DTRA-TR-13-48

12. DISTRIBUTION / AVAILABILITY STATEMENT

Approved for public release; distribution is unlimited.

13. SUPPLEMENTARY NOTES

14. ABSTRACT

For half a century, CdZnTe/CdTe has been investigated for producing radiation detectors. Albeit some success, detector performance and production yield issues remain. Most importantly, the basic science about the factors limiting the detector property and production yield is not understood. The goal of this program is to experimentally and theoretically understand these limiting factors. In addition, techniques will be developed to remove these factors.
In this program, 160 CZT crystals have been grown to achieve the program goal. It is discovered that Cd vacancies and Te antisites (Te at Cd sites) are the two major defects that limit the performance of the CZT/CdTe detectors. The introduction of Zn in to the crystals is one way to reduce the density of Te antisites. A process to reduce Cd vacancies has been developed for the growth of CTZ crystals. Zn has been introduced into the crystals to reduce the densities of the Te antisites. Using these approaches, CTZ with Zn contents of 0%, 4%, 10%, 15%, and 20% have been produced and detectors have been fabricated. The best dectectors are produced in CZT grown with 10% Zn and 1.5% excess Te. The resolution of 57Co 122keV peak is less than 5%.

15. SUBJECT TERMS

radionuclides   detectors   CZT   CdZnTe

16. SECURITY CLASSIFICATION OF:

a. REPORT	b. ABSTRACT	c. THIS PAGE
Unclassified	Unclassified	Unclassified

17. LIMITATION OF ABSTRACT

SAR

18. NUMBER OF PAGES

62

19a. NAME OF RESPONSIBLE PERSON
LTC Thomas Cartledge

19b. TELEPHONE NUMBER (include area code)
N/A

Standard Form 298 (Rev. 8-98)
Prescribed by ANSI Std. Z39.18

CONVERSION TABLE

Conversion Factors for U.S. Customary to metric (SI) units of measurement.

MULTIPLY ⟶ BY ⟶ TO GET

TO GET ⟵ BY ⟵ DIVIDE

angstrom	$1.000\ 000 \times E\ -10$	meters (m)
atmosphere (normal)	$1.013\ 25\ \times E\ +2$	kilo pascal (kPa)
bar	$1.000\ 000 \times E\ +2$	kilo pascal (kPa)
barn	$1.000\ 000 \times E\ -28$	meter^2 (m^2)
British thermal unit (thermochemical)	$1.054\ 350 \times E\ +3$	joule (J)
calorie (thermochemical)	$4.184\ 000$	joule (J)
cal (thermochemical/cm^2)	$4.184\ 000 \times E\ -2$	mega joule/m^2 (MJ/m^2)
curie	$3.700\ 000 \times E\ +1$	*giga bacquerel (GBq)
degree (angle)	$1.745\ 329 \times E\ -2$	radian (rad)
degree Fahrenheit	$t_k = (t°f + 459.67)/1.8$	degree kelvin (K)
electron volt	$1.602\ 19\ \times E\ -19$	joule (J)
erg	$1.000\ 000 \times E\ -7$	joule (J)
erg/second	$1.000\ 000 \times E\ -7$	watt (W)
foot	$3.048\ 000 \times E\ -1$	meter (m)
foot-pound-force	$1.355\ 818$	joule (J)
gallon (U.S. liquid)	$3.785\ 412 \times E\ -3$	meter^3 (m^3)
inch	$2.540\ 000 \times E\ -2$	meter (m)
jerk	$1.000\ 000 \times E\ +9$	joule (J)
joule/kilogram (J/kg) radiation dose absorbed	$1.000\ 000$	Gray (Gy)
kilotons	4.183	terajoules
kip (1000 lbf)	$4.448\ 222 \times E\ +3$	newton (N)
kip/inch^2 (ksi)	$6.894\ 757 \times E\ +3$	kilo pascal (kPa)
ktap	$1.000\ 000 \times E\ +2$	newton-second/m^2 (N-s/m^2)
micron	$1.000\ 000 \times E\ -6$	meter (m)
mil	$2.540\ 000 \times E\ -5$	meter (m)
mile (international)	$1.609\ 344 \times E\ +3$	meter (m)
ounce	$2.834\ 952 \times E\ -2$	kilogram (kg)
pound-force (lbs avoirdupois)	$4.448\ 222$	newton (N)
pound-force inch	$1.129\ 848 \times E\ -1$	newton-meter (N-m)
pound-force/inch	$1.751\ 268 \times E\ +2$	newton/meter (N/m)
pound-force/foot^2	$4.788\ 026 \times E\ -2$	kilo pascal (kPa)
pound-force/inch^2 (psi)	$6.894\ 757$	kilo pascal (kPa)
pound-mass (lbm avoirdupois)	$4.535\ 924 \times E\ -1$	kilogram (kg)
pound-mass-foot^2 (moment of inertia)	$4.214\ 011 \times E\ -2$	kilogram-meter^2 (kg-m^2)
pound-mass/foot^3	$1.601\ 846 \times E\ +1$	kilogram-meter^3 (kg/m^3)
rad (radiation dose absorbed)	$1.000\ 000 \times E\ -2$	**Gray (Gy)
roentgen	$2.579\ 760 \times E\ -4$	coulomb/kilogram (C/kg)
shake	$1.000\ 000 \times E\ -8$	second (s)
slug	$1.459\ 390 \times E\ +1$	kilogram (kg)
torr (mm Hg, 0° C)	$1.333\ 22\ \times E\ -1$	kilo pascal (kPa)

*The bacquerel (Bq) is the SI unit of radioactivity; 1 Bq = 1 event/s.
**The Gray (GY) is the SI unit of absorbed radiation.

Table of Contents

1.0 EXECUTIVE SUMMARY

1.1 Program Goal

For half a century, CdZnTe/CdTe has been investigated for producing radiation detectors. Albeit some success, detector performance and production yield issues remain. Most importantly, the basic science about the factors limiting the detector property and production yield was not understood. The goal of this program was to experimentally and theoretically understand these limiting factors. In addition, techniques will be developed to remove these factors.

1.2 Results – Science

In this program, 160 CZT crystals have been grown to achieve the program goal. It is discovered that Cd vacancies and Te antisites (Té at Cd sites) are the two major defects that limit the performance of the CZT/CdTe detectors. The introduction of Zn into the crystals is one way to reduce the density of Te antisites.

1.3 Results – Detectors

A process to reduce Cd vacancies has been developed for the growth of CZT crystals. Zn has been introduced into the crystals to reduce the densities of Te antisites. Using these approaches, CZT with Zn contents of 0%, 4%, 10%, 15%, and 20% have been produced and detectors have been fabricated. The best detectors are produced in CZT grown with 10% Zn and 1.5% excess Te. The resolution of ^{57}Co 122keV peak is less than 5% at room temperature.

1.4 Future R&D Direction

New approaches to drastically reduce the density of Te antisites are desired for further improving the quality of CZT/CdTe detectors.

1.5 Introduction of this Report

In this report, we put together six papers. These papers were published in five journals, reported in eleven presentations, and printed in four conference proceedings.

2.0   TELLURIUM ANTISITES IN CdZnTe

1. M. Chu, S. Terterian, D. Ting, R.B. James, J.C. Erickson, H.W. Yao, T.T. Lam, M. Szawlowski, and R. Sczeboitz, "Tellurium Antisites in CdZnTe," SPIE Proceedings (Invited Paper), 4507, San Diego, 2001.
2. M. Chu, S. Terterian, D. Ting, R.B. James, J.C. Erickson, H.W. Yao, T.T. Lam, M. Szawlowski, and R. Sczeboitz, "Defect Engineering for Producing High Performance CdZnTe Radiation Detectors," IEEE NSS/MIC Conference (Invited Paper), San Diego, 2001.
3. M. Chu, S. Terterian, D. Ting, S. Mesropian, R.H. Gurgenian, and C.C. Wang, "Tellurium Antisites in CdZnTe," Appl. Phys. Lett. 79, 2728 (2001).

Tellurium antisites in CdZnTe

Muren Chu,[a] Sevag Terterian, David Ting, C. C. Wang, H. K. Gurgenian, and Shoghig Mesropian

Fermionics Corporation, 4555 Runway Street, Simi Valley, California 93063

The electrical properties of CdTe and $Cd_{1-x}Zn_xTe$ crystals grown under excess tellurium by a modified Bridgman technique are critically dependent on the zinc content. Below a value of 0.03, the as-grown CdZnTe crystals are n type while, above this value, CdZnTe crystals are p type. The origin of the shallow donor level at 0.01 eV below the conduction band is most likely singly ionized Te antisites (Te at Cd sites). The origin of the deep donor level at 0.75 eV below the conduction band is therefore doubly ionized tellurium antisites. Based on this model, the conduction type of CdZnTe crystals is determined by the results of compensation between the shallow donors of Te antisites and the shallow acceptors of Cd vacancies. High resistivity $Cd_{1-x}Zn_xTe$ crystals are produced by compensating the p-type crystals with indium impurity at a low doping level of $1-5 \times 10^{15} cm^{-3}$. At room temperature, CdZnTe radiation detectors can resolve the six low energy peaks in the ^{241}Am spectrum, a performance comparable to that of the best CdZnTe detectors reported. © 2001 American Institute of Physics. [DOI: 10.1063/1.1417589]

Because of the large band gap and the abundance of electrons, CdTe has been used for x-ray detectors, gamma ray detectors, and scintillators for many years in spite of many problems with the quality. After the introduction of CdZnTe (CZT), there has been tremendous interest in using this semiconductor system to develop advanced high-sensitivity radiation detectors due to the better detector characteristics of the new material. However, many fundamental properties of the defects, which behave as deep levels and traps in the CdTe–CZT system, are still not well understood. As a result, the production yield of high-performance CZT detectors is still quite low. In this letter, some interesting results are presented and a simple model is proposed as an explanation of the experimental data. In this letter, we also attempt to answer the question of why, over a certain amount of zinc in CZT, the detector performance improves dramatically.[?]

In 1975, Thompson[?] developed a theory to interpret the mechanism for GaAs to exhibit high resistivity. In his theory, deep acceptors with an acceptor level near the middle of the band gap were proposed as the main reason that GaAs reaches high resistivity. When the shallow donors and the shallow acceptors are closely compensated for, the Fermi level is pinned near the deep level and high resistivity semiconductors are produced. Without the deep level, it is very difficult to achieve high resistivity with close compensation between the shallow donors and the shallow acceptors. Similar models have been proposed to interpret the cause of the high resistivity of CdTe.[?] A representative energy level diagram is shown in Fig. 1. In these models, doubly ionized Cd vacancies are assumed to be the deep level acceptors. The simplest compensation between the shallow levels considers column III or column VII elements to be the donors and singly and doubly ionized Cd vacancies to be the acceptors. To further explain the observations that high-density donor impurities

are required for close compensation, vacancy–impurity complexes are introduced into the theory.

The above model for high resistivity CdTe was unanimously accepted until very recently. In 1998, Berding et al.[?] developed a new model that assigned the deep level to Te antisites (Te_{Cd}). This model was based on the observation that the deep level in CZT is actually donors similar to what was reported by Khusnik and Scott[?] in 1991 and based on the theoretical predictions of the stability of Te_{Cd}.[?] In this model, shown in Fig. 1, the deep Te antisite level is located at 0.75 eV below the conduction band, and a shallow donor level of Cl and a shallow acceptor level of copper or other metals are in the CZT crystals for compensation. In 1998, Lee et al.[?] discovered that the high resistivity of CZT was caused by the compensation between a deep donor level and a shallow acceptor level. In 2000, Krsmanovic et al.[?] further experimentally supported the concept of the deep Te_{Cd} donor level.

For this study, $Cd_{1-x}Zn_xTe$ crystals with x values of 0, 0.01, 0.03, and 0.15 were grown repeatedly by a modified Bridgman method. For each growth, excess Te is introduced into the growth melt and, at the end of growth, residual Te on the surface of each crystal is observed. This process assures

CONDUCTION BAND

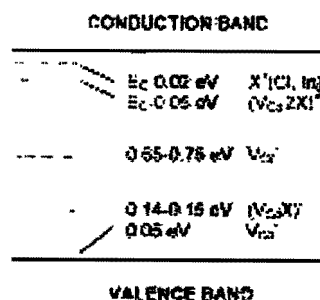|	
E_C 0.02 eV	X^+(Cl, In)
E_C 0.05 eV	$(V_{Cd}2X)^+$
0.65–0.75 eV	V_{Cd}^-
0.14–0.15 eV	$(V_{Cd}X)^-$
0.05 eV	V_{Cd}^-

VALENCE BAND

FIG. 1. Earlier deep level model for high resistivity CdTe.

CONDUCTION BAND

———— Cl

$E_c - 0.75$ eV

Cu

VALENCE BAND
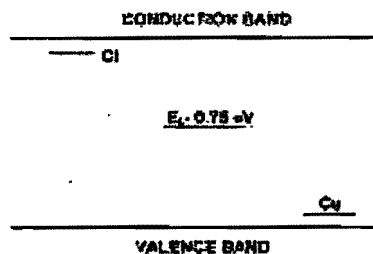
FIG. 2. Deep level model proposed by Fiederle et al. (Ref. 10).

FIG. 3. Electron density of as-grown CdTe as a function of the temperature.

that no Cd interstitials (Cd_i) exist in the crystal. The crystals are of very high quality. The typical etch pit densities (EPDs) for CdTe and $Cd_{0.96}Zn_{0.04}Te$ are on the order of $1-5\times10^4$ and $1-5\times10^4 cm^{-2}$, respectively. The infrared transmissions of the crystals are examined using a Fourier transform infrared (FTIR) spectrophotometer and the measured transmission of 65%–66% for each crystal is near the theoretical limit. The Te precipitates are analyzed using an infrared microscope. Few Te inclusions are observed, indicating very high material quality.[16]

The most important observation seen in the crystals is the electrical properties of the as-grown crystals. Table I lists the measured conduction types and carrier concentrations of the crystals as a function of the Zn content in the crystals. At room temperature, both CdTe and $Cd_{0.96}Zn_{0.04}Te$ are n type and have an electron concentration of the order of low to mid $10^{14} cm^{-3}$. However, $Cd_{0.9}Zn_{0.1}Te$ is p type and has a hole concentration of mid-$10^{15} cm^{-3}$ at room temperature. Between these two groups, $Cd_{0.96}Zn_{0.04}Te$ shows inconsistent results. Some of the crystals are p type while others are n type. Even in the same crystal, the conduction type is not uniform.

The results in Table I have been repeatedly reproduced and, thus, are very reliable. It is then very important to understand the meaning of the information shown in Table I. To investigate the origin of the donors in CdTe and $Cd_{0.96}Zn_{0.04}Te$, a temperature dependent Hall measurement was made on a sample from the as-grown CdTe. The results are shown in Fig. 3. Using the following equation,[17]

$$n = 2(2\pi m^* kT/h^2)^{3/2}[(N_D-N_A)/(gN_A)]\{\exp{-E_D/kT}\}.$$

the donor level is calculated to be 0.01 eV. This shallow donor level is identical to the one assigned to Cd_i^+ or V_{Te}^+ (Te vacancy).[5,18] However, based on the CdTe growth condition that there is residual Te after crystal growth, Cd, and V_{Te} simply cannot exist in our CdTe crystals. Thus, this 0.01 eV donor level must be assigned to some other defect. The most possible point defect remaining as the origin of the donors is then Te antisites. Fiederle et al.'s arguments[10] about the existence of Te_{Cd} applies well here. Combining Fiederle et al.'s results and ours, we therefore assign the origin of the shallow
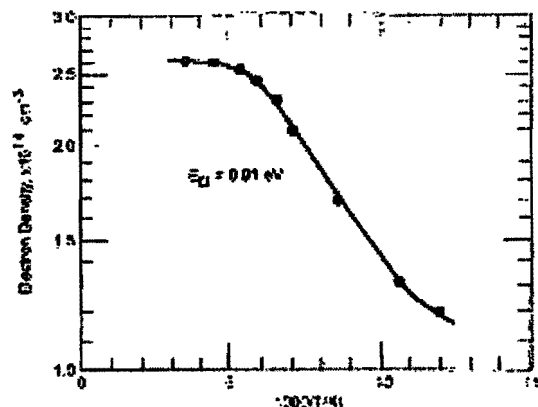
Zn content	0.0	0.04	0.10
Conduction type	n	n or p	p
Carrier density at room temperature (cm^{-3})	$1-5\times10^{14}$	$2-4\times10^{14}$	$4-6\times10^{15}$

donor level 0.01 eV below the conduction band to Te_{Cd}^+, the singly ionized Te antisites, and assign the deep donor level 0.75 eV below the conduction band to Te_{Cd}^{++}, the doubly ionized Te antisites.

Te antisites are actually Te atoms located at Cd vacancies. One can visualize the process of how a CZT crystal becomes Te rich by gradually increasing the Te overpressure supplied by excess Te. In this process, small amounts of Cd vacancies are formed first. As the density of Cd vacancies increases due to the higher Te overpressure, Te atoms begin to occupy some of the vacancy sites. After both the Cd vacancies and Te antisites reach the densities determined by thermodynamics, complexes such as Te precipitates begin to form. Hence, whenever there are Te antisites, Cd vacancies must exist. Therefore, both Te antisites and Cd vacancies exist in CdTe and $Cd_{0.96}Zn_{0.04}Te$ (see Table II). Consequently, the measured carrier densities are results of compensation between Cd vacancies (acceptors) and Te antisites (donors). The low electron densities for CdTe and $Cd_{0.96}Zn_{0.04}Te$ suggest there are slightly more Te antisites than Cd vacancies in these crystals.

The p-type conduction of $Cd_{0.9}Zn_{0.1}Te$ in Table I suggests there are more Cd vacancies than Te antisites in the crystal. A possible explanation for the difference between $Cd_{0.9}Zn_{0.1}Te$ and $Cd_{1-x}Zn_xTe$ with $x=0$ and 0.04 is that when additional Zn is incorporated into the CZT crystals, the lattice parameter is reduced. As a result, the formation energy of Te antisites is higher and the density of Te_{Cd} decreases. Consequently, the $Cd_{0.9}Zn_{0.1}Te$ crystals have more Cd vacancies than Te antisites and become p type. The $Cd_{0.96}Zn_{0.04}Te$ crystals located between the CZT crystals with net donors (CdTe and $Cd_{0.96}Zn_{0.04}Te$) and net acceptors ($Cd_{0.9}Zn_{0.1}Te$) are simply nonuniform and not reproducible as far as the conduction type is concerned.

Based on the above model, if donor impurities are chosen for compensation to produce high resistivity CZT crystals, $Cd_{1-x}Zn_xTe$ with x values over 0.03 are the best candidates. To demonstrate this concept, indium has been introduced into $Cd_{0.9}Zn_{0.1}Te$ crystals. The results show that to produce CZTs with resistivities over $1\times10^{10} \Omega$-cm, the required indium doping level is only $2-3\times10^{15} cm^{-3}$. This doping level is rather close to the room-temperature hole

6

CONDUCTION BAND

In Te_{Cd}^-

Te_{Cd}^{2-}

V_{Cd}

VALENCE BAND

FIG. 4. Proposed deep level defect model.

concentration of mid-10^{12} cm^{-3}, which was measured on $Cd_{1-x}Zn_xTe$ and is listed in Table I. This result is surprisingly different from the reported $1-2\times10^{17}$ cm^{-3} required for producing high resistivity CdTe and CZT. The explanation for this phenomenon is that our CZT crystals have a very small amount of defect complexes to trap indium atoms.

The above results and discussions can be summarized in a very simple model and explained by the energy level diagram shown in Fig. 4. For CdTe and CZT grown with excess Te, Cd vacancies are the shallow acceptors with an acceptor level of 0.05 eV above the valence band. Singly ionized Te antisites are the shallow donors located at 0.01 eV below the conduction band. The relative amount of V_{Cd} and Te_{Cd} depends on the Zn content of the CZT crystal. For $Cd_{1-x}Zn_xTe$ with an x value less than 0.07, the CZT crystals have more Te_{Cd} than V_{Cd} and are n type. For CZT with an x value larger than 0.07, there are more V_{Cd} than Te_{Cd} and the crystals are p type. The doubly ionized Te antisites are the deep donors located at 0.75 eV below the conduction band. The low hole density $Cd_{1-x}Zn_xTe$ can be compensated for with a small amount of indium.

Radiation detectors are fabricated on wafers sliced from the indium doped $Cd_{1-x}Zn_xTe$ ingot. x of island device processing. An energy spectrum measured by a detector the six line energy peaks of X_α, L, Te K, as well as Cd and Te escape peaks, can clearly be identified and the full width at half maximum (FWHM) of the 59.5 keV peak is 4.7 keV. In the ^{57}Co spectrum measured by the same detector, the 136 keV peak beside the 122 keV peak is well resolved and the FWHM of the 122 keV peak is 10.6 keV or 8.7%. These results are comparable to the best reported data.

In summary, the discovery of a shallow donor level

coupled with Fiederle et al.'s demonstration of the existence of Te antisites leads us to propose a very simple defect model to explain the observed electrical properties of the undoped as well as the high-resistivity, indium doped CZT crystals. In the CZT crystals grown with excess Te, Cd vacancies are the dominant shallow acceptors while the singly ionized Te antisites are the dominant shallow donors. The origin of the deep donor level is most likely the doubly ionized Te antisites. For $Cd_{1-x}Zn_xTe$ with an x value less than 0.07, the CZT crystals have more Te_{Cd} than V_{Cd} and are hence n type, while for CZT with an x value larger than 0.07, there are more V_{Cd} than Te_{Cd} and the crystals are p type. When donor impurities such as indium are introduced into CZT to produce a high-resistivity radiation detector material, $Cd_{1-x}Zn_xTe$ with an x value over 0.07 is recommended. The radiation detectors fabricated on the $Cd_{1-x}Zn_xTe$ with a resistivity of more than 5×10^{10} Ω cm exhibit excellent detector characteristics.

[1] Proceedings of the Second International Symposium on Cadmium Telluride: Physical Properties and Applications, Strasbourg, 1976.
[2] See, for example, NSF Proceedings on Hard X-ray Astronomy and Neutron Detector Physics, San Diego, 2000.
[3] Reference in preparation.
[4] A. G. Thompson, J. Electron. Mater. 2, 43 (1973).
[5] D. de Nobel, Philips Res. Rep. 14, 430 (1959).
[6] P. Siffert, A. Cornet, R. Stuck, E. Tabedar, and Y. Marfaing, IEEE Trans. Nucl. Sci. NS-22, 211 (1975).
[7] S. S. Chern and F. A. Kroger, J. Solid State Chem. 14, 44 (1975).
[8] Y. Marfaing, in Ref. 1, p. 223.
[9] R. O. Bell, H. B. Serreze, and F. V. Wald, Proceedings of the Eleventh IEEE Photovoltaics Specialists Conference, New York, 1975, p. 640.
[10] M. Fiederle, C. Eiche, M. Salk, R. Schwarz, K. W. Benz, W. Stadler, D. M. Hofmann, and B. K. Meyer, J. Appl. Phys. 84, 6689 (1998).
[11] M. Khalil, talk in Sect. J, Phys. Condens. Matter 5, 3039 (1993).
[12] M. A. Berding, M. van Schilfgaarde, A. T. Paxton, and A. Sher, Vac. Sci. Technol. A 8, 1103 (1990).
[13] Z. Q. Wang, D. Stroud, and A. J. Markworth, Phys. Rev. B 40, 3129 (1989).
[14] F. A. Lee, J. L. McCleester, R. B. James, R. W. Olsen, H. Hermon, and M. Schieber, Phys. Status Solidi B 113, 000 (1982).
[15] N. Krsmanovic, K. G. Lynn, M. H. Weber, R. Tjossem, N. A. Gundishvili, C. Szeles, E. P. Hong, and L. Chen, Phys. SPIE 3446, 210 (1998).
[16] M. Chu, S. Terterian, D. Ting, C. B. Zarzar, J. C. Lin, and W. H. Yao, Ternary and Multinary Compounds, R. Nordheim, No. SPIE 2507, 000 (1995).
[17] R. H. Bube, Electronic Processes in Crystalline Solids, Academic, New York, 1992.
[18] Yu. N. Rud and K. V. Sanin, Sov. Phys. Semicond. 5, 244 (1971).
[19] S. Lalitha, M. R. Singanelu, and M. A. Chequin, Sov. Phys. Semicond. 8, 83 (1975).

3.0 EFFECTS OF EXCESS Te ON THE PROPERTIES OF CdZnTe RADIATION DETECTORS

1 M. Chu, S. Terterian, D. Ting, C.C. Wang, T. Cartledge, R. Mclaren, J.D. Benson, and J.H. Dinan, "Physics and Chemistry of CdZnTe: from Infrared to Radiation Detection," Military Sensing Symposia on materials, N. Charleston, 2002.

2. M .Chu, S. Terterian, D. Ting, and C.C. Wang, "Defect Physics and Chemistry of CdZnTe: Future Research Direction," Unattended Radiation Sensor Systems for Remote Applications, Washington D.C. 2002.

3. M. Chu, S. Terterian, D. Ting, C.C. Wang, R.B. James, and A. Burger, "Effects of Excess Tellurium on the Properties of CdZnTe Radiation Detectors," J. of Electron Mater. 32, 778 (2003).

4. M. Chu, S. Terterian, D. Ting, C.C. Wang, R.B. James, and A. Burger, "Effects of Excess Tellurium on the Properties of CdZnTe Radiation Detectors," The 2002 U.S. Workshop on the Physics and Chemistry of II-VI Materials, San Diego.

Effects of Excess Tellurium on the Properties
of CdZnTe Radiation Detectors

MUREN CHU,[1] SEVAG TERTERIAN,[1] DAVID TING,[1] C.C. WANG,[1]
J.D. BENSON,[2] J.H. DINAN,[2] R.B. JAMES,[3] and ARNOLD BURGER[4]

1.—Fermionics Corporation, Simi Valley, CA 93063. 2.—US Army RDECOM CERDEC NVESD,
Fort Belvoir, VA 22060. 3.—Brookhaven National Laboratory, Upton, NY 11973. 4.—Fisk
University, Nashville, TN 37208. 5.—E-mail: m.chu@fermionics.com

Room-temperature radiation detectors have been fabricated on high-resistivity,
indium-doped Cd$_{0.9}$Zn$_{0.1}$Te crystals grown under different amounts of excess
Te. The effects of the excess Te on the properties of the detectors are explained
by a simple model using only three parameters: the density of Cd vacancies,
the density of Te antisites (Te at Cd sites), and the deep level of doubly ionized
Te antisites. The best detectors, which can resolve the low-energy Np-L and Te-
K peaks as well as Cd and Te escape peaks of ^{241}Am, are produced from crys-
tals grown with 1.5% excess Te. The detectors fabricated from crystals grown
without excess Te are unable to resolve any characteristic-radiation peaks of
^{241}Am and ^{57}Co. This result is explained by a model of networked p-type do-
mains in an n-type matrix or vice versa, which is caused by the lack of suffi-
cient deep-level Te antisites. Such conduction-type inhomogeneity causes
massive electron and hole trapping. As for the detectors fabricated from
Cd$_{0.9}$Zn$_{0.1}$Te crystals grown with 2% and 3% excess Te, they are able to re-
solve the ^{241}Am 59.5-keV, ^{57}Co 122-keV, and ^{57}Co 136-keV radiation peaks.
However, the full-width at half-maximum (FWHM) values of these peaks
are broadened, especially the high-energy ^{57}Co peaks. These phenomena are
attributed to the hole and, possibly, electron trapping by Cd vacancies and
Te antisites, respectively. The result of the analysis indicates that sufficient Te
antisites and a low density of carrier traps in Cd$_{0.9}$Zn$_{0.1}$Te are essential for
producing high-quality radiation detectors. In the analysis, it was discovered
that most of the excess Te, on the order of 1–2 × 10^{17} cm^{-3}, remain electrically
inactive. A possible explanation for this phenomenon is that the excess Te
atoms form neutral Te-antisite and Cd-vacancy complexes, such as (Te$_{Cd}$·V$_{Cd}$)^2,
during the post-growth cooling process.

Key words: CdZnTe, radiation detector, gamma-ray detector, defect, tellurium
antisite, deep level, cadmium vacancy, inhomogeneity, HgCdTe

INTRODUCTION

Cadmium telluride (CdTe) and cadmium zinc
telluride (CdZnTe) (CZT)) have been considered to
be promising semiconductors for producing room-
temperature radiation detectors for decades.[1] How-
ever, currently the poor production yield in fab-
ricating high-performance detectors using these
materials remains a tremendous issue. The cause of
the problem is that properties of many defects in

these crystals, such as which defects and how the de-
fects affect the detector performance, are not well
understood. In this research, we attempt to develop
a simple physical model to address these questions.

Among the defects in CdTe and CZT, the origin of
the deep-level centers is of particular interest be-
cause these centers are required for producing uni-
form high-resistivity semiconductors.[2] Originally, Cd
vacancies (V$_{Cd}$) were considered to be the dominant
deep-level acceptors.[1,2] Later, it was discovered that
the deep-level centers were actually donors,[3] and the

art jin of the deep-level donors was assigned to Te anti-sites (Te$_{Cd}$).[?] Similar phenomenon was observed in GaAs, and As antisites have been introduced into GaAs to produce high-resistivity materials.[?] Most recently, it was proposed that singly ionized Te anti-sites are shallow-level donors, while doubly ionized Te antisites are the deep-level donors.[?]

Based on the model of deep-level Te antisites,[?] one of the techniques to produce high-resistivity CZT is to first incorporate sufficient Te$_{Cd}$ into the crystals and then to use the shallow-donor impurities, such as indium, to compensate the residual Cd vacancies (the uncompensated amount of V_{Cd} over Te$_{Cd}$). As a result, the Fermi level is pinned to the deep-donor level of the doubly ionized Te antisites, and then, the material becomes highly resistive. In this paper, the quantity of excess Te during the crystal growth is used to control the amount of Te$_{Cd}$ in the crystals; the effects of excess Te in the CZT crystal-growth melt on the radiation-detector performance are reported, and the results are explained by the incorporation of Te$_{Cd}$ and V_{Cd} caused by the excess Te.

EXPERIMENTAL RESULTS

In this study, five groups of Cd$_{0.9}$Zn$_{0.1}$Te crystals were respectively grown by the Bridgman technique using melts with excess Te in the amounts of 0 at.%, 1 at.%, 1.5 at.%, 2 at.%, and 3 at.%. Without impurity doping, all of these crystals are p-type, which is the result of net acceptors of Cd vacancies after the compensation of acceptors of Cd vacancies by the shallow donors of singly ionized Te antisites.[?] To produce CZT with high resistivities, crystals in each of the above five groups were doped with indium (shallow donors) in different quantities until a high resistivity crystal was obtained. The examples of the doping results are shown in Tables I and II. The amount of indium required for producing high-resistivity CZT needs to be controlled very precisely. The reproducibility of the high resistivity is also demonstrated.

The indium concentration introduced to achieve a high resistivity for each of the five groups is shown in Table III. The crystals that have not been fabricated into detectors, such as Crystal 9971, are not included in this table. The data clearly shows that

the indium density needed for obtaining a high-resistivity crystal is proportional to the magnitude of the excess Te in the crystal-growth melt. For Crystal 9294, grown without excess Te, a very low indium concentration on the order of 2×10^{14} cm^{-3} is sufficient to compensate the residual-Cd vacancies to achieve a high resistivity. As the amount of excess Te increases, more indium is required for compensating the residual-Cd vacancies. This phenomenon indicates that a CZT crystal has more net Cd vacancies as the crystal is grown with more excess Te.

Radiation detectors, with a size of $4 \times 4 \times 1$ mm^3 to $6 \times 6 \times 3$ mm^3, were fabricated in wafers from each of the five crystals listed in Table III and were subsequently tested using radiation sources of ^{57}Co and ^{241}Am. The testing results are also summarized in Table III. Evidently, the Cd$_{0.9}$Zn$_{0.1}$Te-detector performance critically depends on the amount of excess Te added into the crystal-growth melts. The detectors fabricated from Crystal 9294, which was grown without excess Te, cannot resolve any of the radiation peaks of ^{57}Co and ^{241}Am. Instead, a random broad peak was observed. A ^{57}Co spectrum, measured by these detectors, is shown in Fig. 1. This observation is consistent with the fact that there is no reported detection result on detectors fabricated in CZT/CdTe grown without excess Te. The detectors from Crystal 9489, which was grown with 1% excess Te, have better performance and can resolve the ^{57}Co 122-keV and ^{241}Am 59.5-keV peaks. The best detectors among those listed in Table III are fabricated from CZT 9364, a crystal grown with 1.5% excess Te. The ^{241}Am and ^{57}Co spectra measured by these detectors are shown in Figs. 2 and 3, respectively. In addition to the ^{57}Co 122-keV, ^{57}Co 136-keV, and ^{241}Am 59.5-keV peaks, the detectors can also resolve the six low-energy X-peaks: Te-K, Cd-escape, and Te escape peaks. Besides, the full-widths at half-maximum (FWHM) values of the ^{57}Co 122 keV and ^{241}Am 59.5-keV peaks have very low values of 8.2 keV and 4.2 keV, respectively.

When more than 1.5% excess Te is introduced into the CZT growth melt, good detectors can still be fabricated from the grown crystal, but the performance of the detectors begins to degrade. As shown in Table III, the degree of degradation is proportional to the amount of the excess Te used for the CZT

Table I. Indium Doping Results in CdZnTe (10% Zn) Grown with 0% Excess Te

Indium Level (cm^{-3})	Crystal Log Number	Conduction Type	Resistivity (Ω·cm)
0	9161	P	2 × 10$^?$
1.2 × 10^{14}	9146	P	9 × 10$^?$
2.0 × 10$^?$	9159	P	6 × 10$^?$
2.1 × 10$^?$	9291	N	8 × 10$^?$
2.7 × 10^{14}	9452	N	1 × 10$^?$
4.3 × 10$^?$	9205	N	5 × 10$^?$
7.4 × 10^{14}	9296	N	6 × 10$^?$
9.6 × 10$^?$	9221	N	7.5 × 10$^?$

Table II. Indium Doping Results in CdZnTe (10% Zn) Grown with 1.5% Excess Te

Indium Level (cm^{-3})	Crystal Log Number	Conduction Type	Resistivity (Ω·cm)
1.2 × 10^{15}	9294	P	1 × 10$^?$
2.5 × 10^{15}	9354	P	2 × 10$^?$
2.6 × 10^{15}	9572	P	2 × 10$^?$
2.8 × 10^{15}	9572	P	5 × 10$^?$
3.0 × 10^{15}	9228	N	1 × 10$^?$
4.2 × 10^{15}	9379	N	6 × 10$^?$
8.4 × 10^{16}	9216	N	0.7 × 10^{-1}

Table III. Properties of Cd$_{1-x}$Zn$_x$Te Crystals and Detectors as a Function of Excess Te in Crystal-Growth Melt

Stoichiometry (Te/(Cd + Zn))	1.000	1.010	1.016	1.020	1.030
Crystal log number	9254 9262	9489	9364 9372	9616	9258
Resistivity (Ω cm)	10^{9}	10^{9}	$\geq 10^{9}$	$\sim 10^{9}$	$\times 10^{9}$
Indium doping (cm^{-3})	2.1×10^{14}	3.3×10^{15}	2.5×10^{15}	6.1×10^{15}	1×10^{16}
^{57}Co 122-keV peak	X	Resolved	8.2 keV	13.4 keV	Resolved
^{57}Co 136 keV peak	X	X	Resolved	Resolved	Resolved
FWHM of ^{241}Am, 59.5 keV	X	Resolved	6.7 keV	6.5 keV	6.6 keV
Np-L, Te-K, Cd, and Zn escape peaks from ^{241}Am	X	X	Resolved	X	X

*X denotes not resolved.
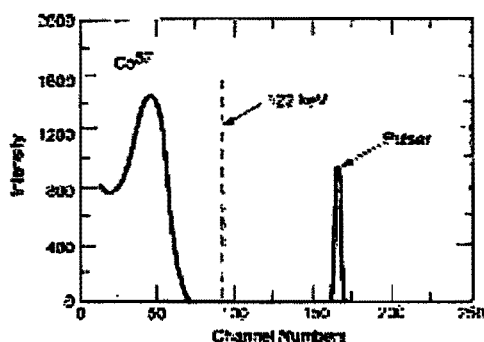
Fig. 1. The spectrum of ^{57}Co measured by detectors (4 × 4 × 1 mm^3) 105 V from CZT 9254
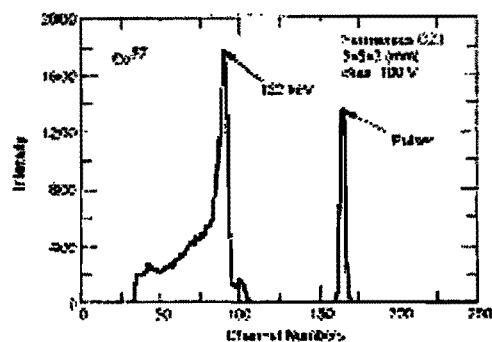
Fig. 3. The spectrum of ^{57}Co measured by detectors from CZT 9364
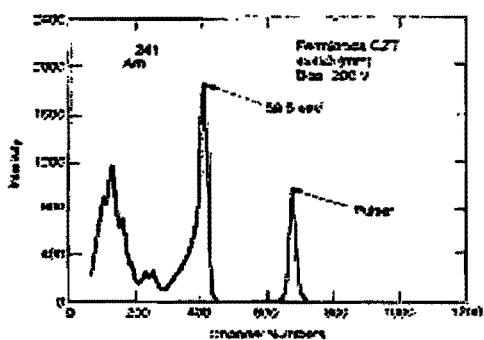
Fig. 2. The spectrum of ^{241}Am measured by detectors from CZT 9361
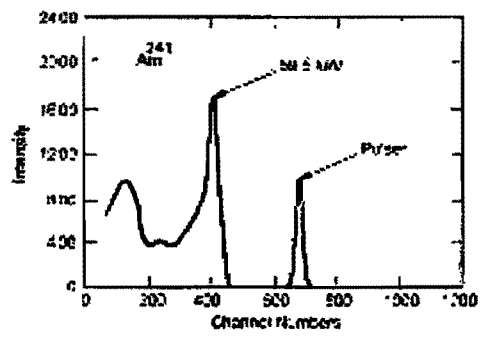
Fig. 4. The spectrum of ^{241}Am measured by a detector (4 × 4 × 1 mm^3) 105 V from CZT 9258

growth. Detectors from CZT 9616, which were grown with 2% excess Te, can resolve the major ^{57}Co and ^{241}Am peaks. The values of the FWHM of the ^{57}Co 122-keV and ^{241}Am 59.5-keV peaks are still respectable. The detectors can detect the envelope of the low energy ^{241}Am 59.5-keV peaks but cannot distinguish the individual peaks. The characteristics

of detectors from CZT 9258, a crystal grown with 3% excess Te, are even worse. Figures 4 and 5 show, respectively, the ^{241}Am and ^{57}Co spectra measured by one of these detectors. There is a low end shoulder to the left side of the ^{57}Co 122-keV peak, a typical sign of carrier trapping. As a result, a meaningful FWHM value of this peak cannot be measured.

11
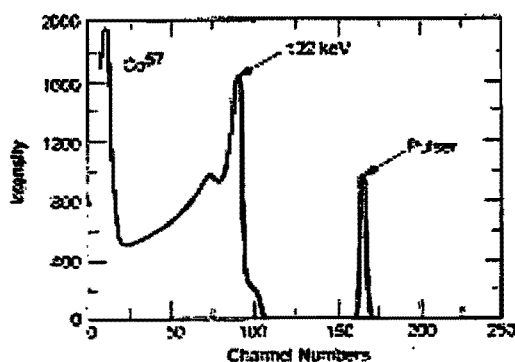
Fig. 5. The spectrum of [57]Co measured by a detector (4 × 4 × 1 mm³) fabricated from CZT 9238

DISCUSSION

Theoretical Model

From the preceding effects of excess Te on the properties of $Cd_{0.9}Zn_{0.1}Te$ radiation detectors, a simple semiquantitative theoretical model, using only defects of Cd vacancies and Te antisites, is developed for the understanding of the experimental results. To construct this model, the indium concentration in Table III is first drawn in Fig. 6 as a function of the excess Te. This curve is then considered to be the concentration curve of uncompensated-Cd vacancies (difference of V_{Cd} and Te_{Cd}) because the high resistivity of each CZT crystal is achieved by compensating the residual V_{Cd} by indium. From the limited data, a precise curve of Te_{Cd} as a function of excess Te cannot be obtained. However, it is possible to draw a semiquantitative curve of the Te_{Cd} distribution. First, the Te_{Cd} concentration of 1×10^{16} cm⁻³,
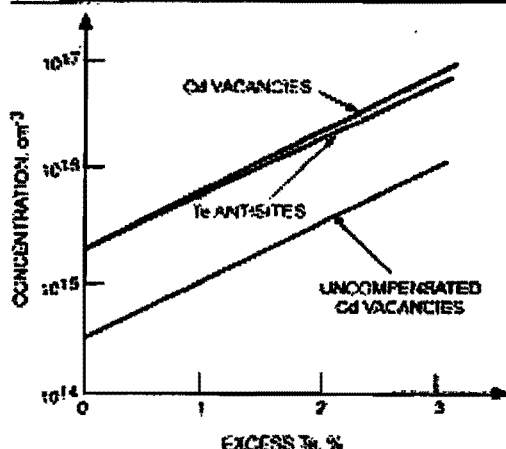
Fig. 6. The semiquantitative defect concentration curves constructed for explaining the experimental results in Table III.

approximated by Fiederle et al.[3] is assigned to CZT 9234, from which the best detectors were fabricated. Second, it is obvious that the concentration of the Te_{Cd} increases monotonically with the amount of excess Te in the CZT-growth melts. Then, the Te_{Cd} concentration curve as a function of the excess Te, a curve with a positive slope, can be drawn in Fig. 6. The undetermined variable is the precise value of the slope of this curve. The Cd-vacancy concentration curve is simply the sum of the other two. Using the information in Fig. 6, the detector performance data as a function of the excess Te can readily be explained.

Conduction-Type Inhomogeneity

The [57]Co spectrum measured by detectors from CZT 9234 is shown in Fig. 1. None of the characteristic [57]Co peaks is observed. Instead, there is a broad peak with energy much lower than the 122 keV. This result is explained by a model of networked p-type domains in an n-type matrix or vice versa, which is caused by the lack of sufficient deep-level Te antisites or Cd vacancies. Such conduction-type inhomogeneity causes massive electron and hole trapping. This model is similar to the one developed for HgCdTe[11] and is published elsewhere.[12]

Optimal CdZnTe Detectors

The excellent detection results of detectors from CZT 9234 suggest that this crystal has sufficient deep-level Te antisites to pin the Fermi level to the middle of the bandgap and has a minimal amount of carrier traps. Therefore, the detectors can resolve the low-energy [241]Am peaks and exhibit low FWHM of the two low-γ peaks of [57]Co and [241]Am. These results indicate that to incorporate sufficient Te antisites in CZT for reaching a high resistivity, excess Te in the amount of 1.5% or in its neighborhood needs to be introduced into the growth melt for the CZT growth. To produce even better detectors, ingenious methods to further control the concentrations of deep-level defects/impurities and carrier traps need to be developed.

The amount of excess Te for the growth of CZT 9489 is between those for CZT 9234 and CZT 9364. The fact that the detectors from this crystal can resolve the [57]Co 122-keV peak but not the 136-keV peak indicate that the performance of these detectors are also between those of CZT 9234 and CZT 9364. These phenomena can be explained by the concept that the slightly insufficient concentration of the deep-level Te antisites in this crystal, shown in Fig. 6, still leaves a certain amount of conduction-type inhomogeneity in the crystal.

Hole Trapping by V_{Cd} and Electron Trapping by Te_{Cd}

Figures 4 and 5 are, respectively, the spectra of [241]Am and [57]Co measured by detectors from CZT 9238. The severe degradation of the 122-keV peak to the degree that its FWHM cannot be measured

12

indicates a high degree of hole and, possibly, electron trapping. Comparing these results with the curves shown in Fig. 6, the hole trapping is caused by a high density of Cd vacancies and the electron trapping by Te antisites. The effects of the hole/electron trapping to the low-energy ^{241}Am gamma rays are that the FWHM of these peaks are broadened to the degree that each individual peak cannot be distinguished from the others, but the overall envelop can still be observed. The higher degree of degradation of the 122 keV ^{57}Co peak than the ^{241}Am 59.5-keV peak suggests that hole trapping plays the major role in the trapping mechanism.

The amount of excess Te for CZT 9618 is between these for crystals 9564 and 9238. Based on the Cd vacancy and Te antisite curves shown in Fig. 6, the properties of the detectors from CZT 9618 will also be between the properties of detectors from CZTs 9564 and 9238. The measured results are in agreement with this prediction. There are broadening of the FWHM of all the peaks compared to the spectra measured by detectors from CZTs 9564 and 9572, but the FWHM of the ^{57}Co 122-keV peak can still be measured.

Possibility of Te-Related Neutral Defects

An interesting observation of the preceding discussion is that the concentrations of electrically active Cd vacancies and Te antisites are on the order of 10^{12}–10^{14} cm^{-3}, while the concentration of the excess Te atoms in the CZT crystals is on the order of 1–2×10^{17} cm^{-3}. An explanation is that, at the growth temperature of 1,100°C, most of the excess Te is incorporated into the CZT crystals in the form of Cd vacancies and Te antisites. One Cd vacancy can be considered as one excess Te atom, and one Te antisite can be considered as two excess Te atoms. During the cooling process after the growth, the high densities of Cd vacancies and Te antisites on the order of 10^{17} cm^{-3} must be reduced because of the low solubility of these defects at lower temperatures. In this process, neutral defect species in a high concentration are formed. The simplest form of the neutral species will be Te$_{Cd}$+V$_{Cd}$, a complex formed by one Te antisite and two Cd vacancies. This complex, equivalent to four excess Te atoms, can serve as a nucleation center for the formation of more complicated defects, such as Te precipitates.

CONCLUSIONS

It is demonstrated that the performance of Cd$_{1-x}$Zn$_x$Te radiation detectors are critically dependent on the amount of excess Te in the growth

melt. A semiquantitative theoretical model based only on Te antisites and Cd vacancies is proposed to explain all of the observed experimental results. With low excess Te of 1% or less, the CZT crystals have insufficient Te$_{Cd}$ to provide deep-level donors to pin the Fermi level at the middle of the bandgap. As a result, p-type domains are formed in an n-type matrix or n domains in a p matrix. This conductivity-type inhomogeneity causes massive electron and hole trapping. Consequently, the detectors are unable to resolve the radiation peaks. With an excess Te of 2% or more, the high concentration of ionized Cd vacancies and Te antisites serve, respectively, as hole traps and electron traps, which degrade the resolution of the CZT detectors. The best detectors are produced from CZT crystals grown with an intermediate amount of excess Te of 1.5%, which has sufficient Te$_{Cd}$ to pin the Fermi level to the middle of the bandgap and has no excessive amount of defects to trap charge carriers. It was also found that most of the excess Te atoms are not electrically active. It is proposed that they exist in the form of neutral-defect complexes, such as Te$_{Cd}$(V$_{Cd}$)$_2$.

REFERENCES

1. Papers presented at Proc. 12th Int. Symp. on Cadmium Telluride Physical Properties and Applications, Strasbourg, 1976.
2. A.G. Thompson, J. Electron. Mater. 2, 471 (1973).
3. D. de Nobel, Philips Res. Rep. 14, 430 (1959).
4. G.M. Khattak and C.G. Scott, J. Phys. Condens. Matter 3, 8619 (1991).
5. M. Fiederle, C. Eiche, M. Salk, R. Schwarz, K.W. Benz, W. Stadler, D.M. Hofmann, and B.K. Meyer, J. Appl. Phys. 84, 6689 (1998).
6. R.Y. Lee, J.L. Melvin, R.B. James, R.W. Olsen, H. Hermon, and M. Schieber, Proc. SPIE 3768, 115 (1999).
7. N. Krsmanovic, K.G. Lynn, M.H. Weber, R. Tjossem, S.A. Awadalla, C. Szeles, C.P. Flint, and J.L. Glass, Proc. SPIE 4141, 230 (2000).
8. D.S. Holmes, R.T. Chen, K.R. Elliott, and C.G. Kirkpatrick, Appl. Phys. Lett. 40, 181 (1982).
9. M.C. Flynn and D.V. Morgan, eds., Gallium Arsenide Materials, Devices, and Circuits (New York: John Wiley & Sons, 1985), pp. 60–85.
10. M. Chu, S. Terkelsen, D. Ting, C.C. Wang, H.K. Gurgenian, and S. Vasquez, Appl. Phys. Lett. 79, 2728 (2001).
11. M.C. Chen, S.C. Beton, and D.F. Weirauch, J. Appl. Phys. 63, 3327 (1988).
12. M. Chu, S. Terkelsen, D. Ting, R.B. James, M. Szawlowski, and G.J. Visser, Proc. SPIE 4784 (2002).

4.0 EFFECTS OF P/N INHOMOGENEITY ON CdZnTe RADIATION DETECTORS

1. M. Chu, S. Terterian, D. Ting, R.B. James, M. Szawlowski, and G.J. Visser, "Effects of p/n Inhomogeneity on CdZnTe Radiation Detectors," SPIE Proceedings, Vol. 4784A, 237, Seattle, 2002.

Effects of p/n Inhomogeneity on CdZnTe Radiation Detectors

M. Chu,* S. Terterian, D. Ting, R.B. James,[a] M. Szawlowski,[b] and G.J. Visser[c]

Fermionics Corporation
4555 Runway St, Simi Valley, CA 93063

[a] Brookhaven National Laboratory; [b] Advanced Photonix, Inc.; [c] Nova R&D, Inc.

ABSTRACT

Spectrometer grade, room-temperature radiation detectors have been produced on $Cd_{0.90}Zn_{0.10}Te$ grown by the low-pressure Bridgman technique. Small amount of indium has been used to compensate the uncompensated Cd vacancies for the crystals to be semi-insulating. The properties of the detectors are critically dependent on the amount of excess Te introduced into the growth melts of the $Cd_{0.90}Zn_{0.10}Te$ crystals and the best detectors are fabricated from crystals grown with 1.5% excess Te. Detector resolution of ^{57}Co and ^{241}Am radiation peaks are observed on all detectors except the ones produced on $Cd_{0.90}Zn_{0.10}Te$ grown from the melt in the stoichiometric condition. The lack of resolution of these stoichiometric grown detectors is explained by a p/n conduction-type inhomogeneity model.

Keywords: CdTe, CdZnTe, Radiation Detectors, Gamma Ray Detectors, Defects, Te Antisites.

1. INTRODUCTION

CdTe and CdZnTe (CZT) have been considered to be promising semiconductors for producing room temperature radiation detectors for decades.[1] However, the only high quality room-temperature CdTe/CZT detectors are fabricated from $Cd_{0.80}Zn_{0.20}Te$ grown under a high pressure condition.[2] In this paper, we report the properties of spectrometer grade $Cd_{0.90}Zn_{0.10}Te$ detectors produced on low-pressure grown crystals. The detector testing results as a function of excess Te in the crystal growth melts are described in Section 2. The poor resolution of detectors fabricated from crystals grown from stoichiometric melts is explained by an inhomogeneity model in Section 3.

2. EXPERIMENTAL RESULTS

In this study, five groups of $Cd_{0.90}Zn_{0.10}Te$ crystals were respectively grown by the low pressure Bridgman technique using melts with excess Te in the amounts of 0.0, 1.0, 1.5, 2.0, and 3.0 atomic percent. Without impurity doping, all of these crystals are p-type, which is the result of net acceptors of Cd vacancies after the compensation of acceptors of Cd vacancies by the shallow donors of singly ionized Te antisites.[3] To produce CZT with high resistivities, crystals in each of the above five groups were doped with indium (shallow donors) in different quantities until a high resistivity crystal was obtained. The amount of indium required for producing high resistivity CZT needs to be controlled very precisely. The reproducibility of the high resistivity is about 75%.

The indium concentration introduced into the crystals for achieving a high resistivity for each of the five groups is shown in Table I. The data clearly shows that the indium density needed for obtaining a high resistivity crystal is proportional to the magnitude of the excess Te in the crystal growth melt. For Crystal 9294, grown without excess Te, a very low indium concentration on the order of $2x10^{14}$ cm^{-3} is sufficient to compensate the residual Cd vacancies to achieve a high resistivity. As the amount of excess Te increases, more indium is required for compensating the residual Cd vacancies. This phenomenon indicates that a CZT crystal has more net Cd vacancies as the crystal is grown with more excess Te.

---

* E-mail: M.Chu@Fermionics.com

Table I. Properties of $Cd_{0.90}Zn_{0.10}Te$ crystals and detectors as a function of excess Te in crystal growth melt. "X" denotes "not resolved."

Stoichiometry (Te/(Cd+Zn))	1.000	1.010	1.015	1.020	1.030
Crystal Log #	9294	9489	9872	9618	9238
Resistivity ($\Omega \cdot cm$)	10^8	10^8	$\geq 10^9$	$\geq 10^9$	$\geq 10^9$
Indium-doping (cm^{-3})	2.1×10^{14}	3.3×10^{15}	2.5×10^{15}	6.4×10^{15}	1×10^{16}
^{57}Co 122 keV Peak	X	Resolved	6.0 keV	13.4 keV	Resolved
^{57}Co 136 keV Peak	X	X	Resolved	Resolved	Resolved
FWHM of ^{241}Am @ 59.5 keV	X	Resolved	3.6 keV	6.5 keV	6.6 keV
Np-L, Te-K, Cd and Te Escape Peaks From ^{241}Am	X	X	Resolved	X	X

Radiation detectors, with sizes between 4x4x1 mm^3 and 5x5x3 mm^3, were fabricated in wafers from each of the five crystals listed in Table I and were subsequently tested using radiation sources of ^{57}Co and ^{241}Am. The testing results are also summarized in Table I. Evidently, the $Cd_{0.90}Zn_{0.10}Te$ detector performance critically depends on the amount of excess Te added into the crystal growth melts. The detectors fabricated from Crystal 9294, which was grown without excess Te, cannot resolve any of the radiation peaks of ^{57}Co and ^{241}Am. Instead, a random broad peak was observed. A ^{57}Co spectrum measured by these detectors is shown in Figure 1. This observation is consistent with the fact that there is no reported room-temperature detection result on detectors fabricated in CZT/CdTe grown without excess Te.
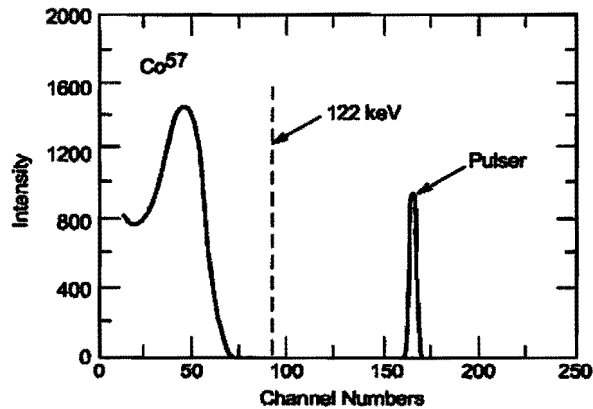
Figure 1. Spectrum of ^{57}Co measured by detectors (4x4x1 mm^3, 100V) from CZT 9294.

The detectors from Crystal 9489, which was grown with 1% excess Te, have better performance and can resolve the ^{57}Co 122 keV and ^{241}Am 59.5 keV peaks. The best detectors among those listed in Table I are fabricated from CZT 9364, a crystal grown with 1.5% excess Te. The ^{241}Am and ^{57}Co spectra measured by these detectors are shown in Figures 2 and 3, respectively. In addition to the ^{57}Co 122 keV, ^{57}Co 136 keV, and ^{241}Am 59.5keV peaks, the detectors can also resolve the six ^{241}Am low energy Np-L, Te-K, Cd-escape, and Te-escape peaks. Besides, the full widths at half maximum (FWHM) of the ^{57}Co 122 keV and ^{241}Am 59.5keV peaks have very low values of 6.0 keV and 3.6 keV, respectively.

When more than 1.5% excess Te is introduced into the CZT growth melt, detectors with the capability of resolving the radiation peaks can still be produced from the grown crystal; but the performance of the detectors begin to degrade. As shown in Table I, the degree of degradation is proportional to the amount of the excess Te

16

used for the CZT growth. Detectors from CZT 9618, which were grown with 2.0% excess Te, can resolve the major ^{57}Co and ^{241}Am peaks. The values of the FWHMs of the ^{57}Co 122 keV and ^{241}Am 59.5keV peaks are still respectable. But the detectors can detect only the envelop of the low energy ^{241}Am 59.5keV peaks instead of the individual ones. The characteristics of detectors from CZT 9238, a crystal grown with 3.0% excess Te, are even worse. There is a broad shoulder to the left side of the ^{57}Co 122 keV peak, a typical sign of high hole trapping. As a result, a meaningful FWHM value of this peak cannot be measured.
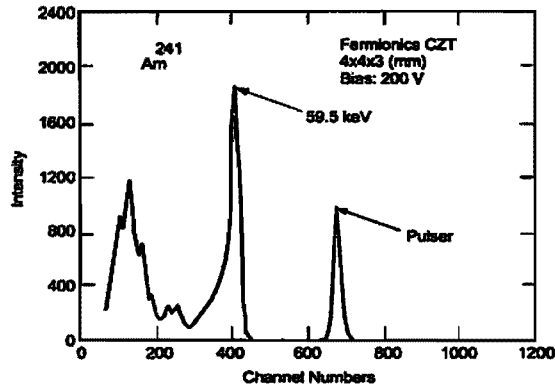
Figure 2. Spectrum of ^{241}Am measured by a detector from CZT 9872.
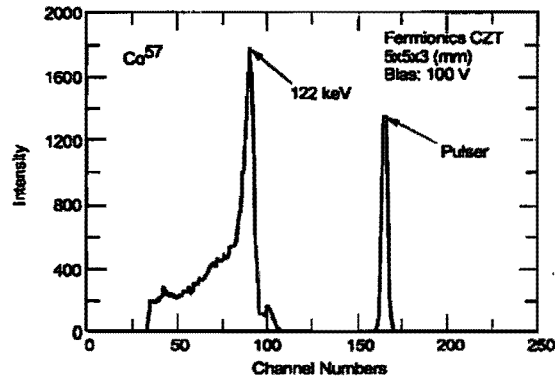
Figure 3. Spectrum of ^{57}Co measured by a detector from CZT 9364

3. DISCUSSIONS

The discussion of the general properties of the detector results in Table I will be published elsewhere. In this paper, the discussion will be focused on detectors from CZT 9294. The ^{57}Co spectrum measured by these detectors from is shown in Figure 1. None of the characteristic ^{57}Co peaks is observed. Instead, there is a broad peak with energy much lower than the 122 keV. To understand the cause of such results, a separate experiment was conducted. Several detectors from CZT 9294 and CZT 9364 were exposed to visible light and the DC and low frequency photocurrent from each detector was measured. All detectors from CZT 9294 have photocurrents more than twenty times higher than those measured on the well-behaved detectors from CZT 9364. How can CZT 9294 detectors that cannot resolve gamma ray peaks show such peculiar high photocurrents to visible light? For such high currents, the hole lifetime in CZT must be higher than an unheard value of 20 μsec. To explain these results, a model[4] proposed on small bandgap, near intrinsic HgCdTe can be used.

17

In low carrier concentration ($\sim 10^{14}$ cm^{-3}) n-type HgCdTe with a cutoff wavelength of $\sim$12 μm, extended p-type inclusions or domains are frequently observed.[5] Dislocations are a potential cause of the p-type domains. In near intrinsic n-type material, a small amount of acceptor impurities or defects ($\geq 1 \times 10^{14}$ cm^{-3}) diffused through dislocations can easily convert the neighborhood of the dislocations to p-type. The symptoms of such a structure are a higher than normal DC and low frequency photocurrent in photoconductors larger than 1 mm, and an unreasonably high measured hole lifetime. The model[4] developed to explain these phenomena states that the extended p-type domains in the n-type matrix form a potential well for holes. When the p-type domains form a network connected to the cathode, a new mechanism to collect the holes is formed: the photo-generated holes in the n-type matrix can drift into the potential well and be collected. This process is illustrated in Figure 4. In a conventional n-type HgCdTe photoconductor with no p-type domain, as shown in Figure 4(a), holes that can be collected by the cathode must be generated within a distance of $l_h = \mu_h \tau_h E$ from the cathode, where μ_h is the hole mobility, τ_h is the hole lifetime, and E is the electric field. But in n-type HgCdTe with networked p-type domains connected to the cathode, the situation is different. Since the holes in the p-type potential well have fewer electrons to recombine with, they can have a very long apparent (measured) lifetime (τ_h^{in}) and drift for a very long distance l_h^{in}, where "in" denotes "inhomogeneity". Consequently, as shown in Figure 4(b), holes generated by the photons outside the l_h range from the cathode can still be collected by drifting into the p-type domains and then to the cathode. As a result, the photoconductor can collect a higher photocurrent. It is noted though that the detectivity of such detectors actually suffers because the detector leakage current and noise are very high.
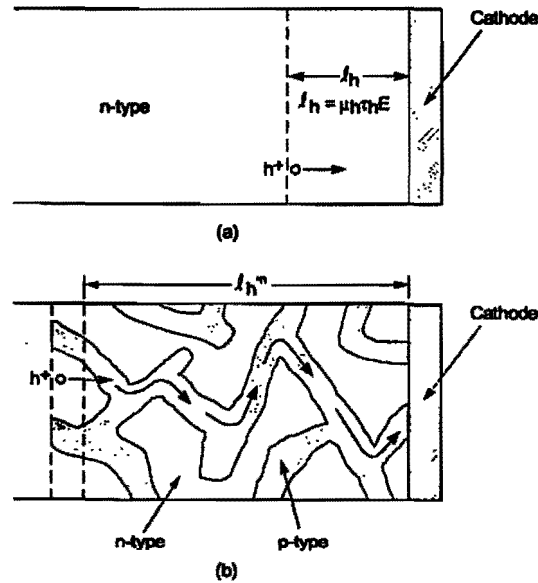
Figure 4. Modeling of DC collection of photo-generated holes in near intrinsic n-HgCdTe: (a) homogeneous condition, and (b) inhomogeneous condition with p-networks in n-matrix.

The phenomenon of the peculiar high photocurrent in response to visible light observed on detectors from CZT 9294 is similar to the excess high photocurrent and unreasonable high carrier lifetime found on the HgCdTe photoconductors with p/n inhomogeneity. According to the model explained by Figure 4, CZT 9294 may also have networked p-type domains in an n-type matrix. This idea is consistent with the fact that CZT 9294 was grown from stoichiometric melt. Comparing CZT 9294 with other crystals in Table I, this crystal has the least amount of Cd vacancies and Te antisites, the defects been proposed as the deep levels to pin the Fermi level to the center of the bandgap. According to Ref. 5 and 6, it is impossible to achieve homogeneous high resistivity simply by close compensation between shallow donors and acceptors. Any slight fluctuation of the densities of acceptors and donors can cause conduction-type inhomogeneity. For achieving high resistivity, a semiconductor must have sufficient

impurities or defects with a deep level near the middle of the bandgap to pin the Fermi level to it. Based on the above discussion, it becomes clear that the density of deep level Te antisites or Cd vacancies in CZT 9294 has reached such a low level that p-type networks has formed in the n-type matrix.

The concept of conduction-type inhomogeneity can be used to well explain the measured gamma ray spectrum shown in Figure 1. The model of this explanation is illustrated in Figure 5. During the measurements, the shaping time (t_s) is typically 1-2 μsec and is comparable to the hole lifetime τ_h. In a detector without conduction-type inhomogeneity, the holes generated in a distance of $l_h(t_s) = \mu_h t_s E$ from the cathode are collected within the shaping time after receiving a gamma ray photon. However, in a detector with networks of p-domains in n-matrix, many holes are collected by first drifting from the n-matrix to branches of the p-domains, and then to the cathode. Since in the p-type networks the holes travel through zigzag channels, and the maximum hole traveling distance is l_h (t_s), the holes that can be collected in the shaping time t_s after a gamma ray photon reaches the detector are then in a distance of l_h' from the cathode, which is shorter than the distance of $l_h(t_s)$. As a result, detectors from CZT 9294 collect much less holes in t_s than a homogeneous detector does in the same time period, and will consider the incident gamma ray to have a lower energy than it actually has. Furthermore, in the following shaping time periods, even if there is no incident gamma ray, holes generated by the original gamma ray in the area beyond the distance of l_h' from the cathode are still collected through the p-channels. As a result, when a detector from CZT 9294 receives 122 keV gamma ray photons, the electronics does not register single gamma ray photons with this energy. Instead, it registers a number of low energy gamma ray photons. Thus, Figure 1 curve is formed and no characteristic [57]Co peak is observed.

The relationship between l_h' and $l_h(t_s)$ can be approximated by considering the averages of these parameters. Assuming l_p is the average distance the holes travel in the p-channel in t_s, then

$$l_h' = \alpha \, l_p \tag{1}$$

where α is a constant less than 1. Let E' be the average electric field in the p-channel along the velocity of the holes and E be the electric field in Figure 5(a), then

$$E' = \alpha E \tag{2}$$

Substituting $l_p = \mu_h t_s E'$ and Eq.2 to Eq.1, and use $l_h(t_s) = \mu_h t_s E$,

$$l_h' = \alpha^2 l_h(t_s) \tag{3}$$

Since the orientation of each branch of the p-channel is random, the average orientation of l_p can be approximated to be 45° from the orientation of l_h', and α becomes cos45°. Then, Equation (3) becomes

$$l_h' = l_h(t_s)/2 \tag{4}$$

In homogeneous CZT detectors, most of the holes contributed to the 122 keV peak in a [57]Co spectrum are generated and collected in the region within the distance of $l_h(t_s)$ from the electrode. Now, in the inhomogeneous CZT detectors, these holes are still generated in this region, but they will be collected in two consecutive shaping times because of Equation 4. Therefore, it is expected that in the spectrum of inhomogeneous detectors, the [57]Co 122 keV gamma ray will register near 61 keV. And this is exactly what is observed in Figure 1. Naturally, for different degree of inhomogeneity, the [57]Co peak will shift accordingly.

The model described by Figure 5 presents the hole "trapping" effect. By the same argument, the "trapping" effect applies to electrons too. Here, Figure 5 discussed the "trapping" mechanism by the extended routs for holes and electrons to travel. Another massive trapping mechanism in the p/n inhomogeneity is the trapping of carriers by isolated potential wells, which can be easily understood and doesn't need to be elaborated.
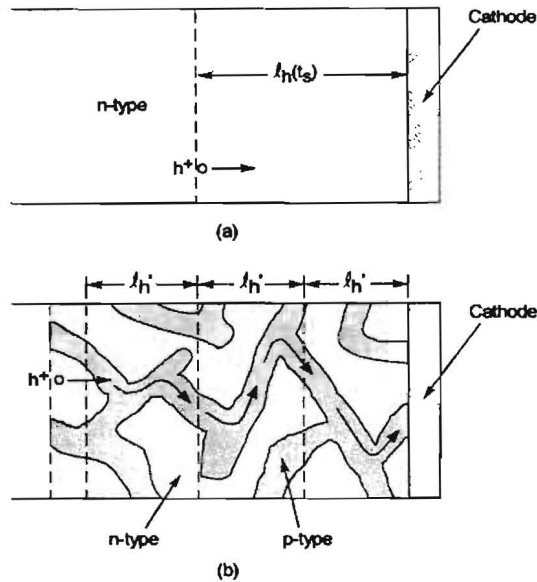
19

Figure 5. Modeling of gamma ray spectral response by CZT detectors
In (a) homogeneous condition, and (b) inhomogeneous condition with
p-networks in n-matrix.

4. SUMMARY

In summary, Spectrometer grade, room-temperature radiation detectors have been produced on $Cd_{0.90}Zn_{0.10}Te$ grown by the low-pressure Bridgman technique. Small amount of indium has been used to compensate the uncompensated Cd vacancies for the crystals to be semi-insulating. The properties of the detectors are critically dependent on the amount of excess Te introduced into the growth melts of the $Cd_{0.90}Zn_{0.10}Te$ crystals and the best detectors are fabricated from crystals grown with 1.5% excess Te. Detector resolution of [57]Co and [241]Am radiation peaks are observed on all detectors except the ones produced on $Cd_{0.90}Zn_{0.10}Te$ grown from the melt in the stoichiometric condition. The lack of resolution of these stoichiometric grown detectors is explained by a p/n conduction-type inhomogeneity model. Because of the lack of excess Te, such crystals do not have sufficient Cd vacancies and Te antisites, the deep level species, to pin the Fermi level to the middle of the bandgap. As a result, p-type domains in n-type matrix or vice versa are formed. Such inhomogeneity causes trapping of electrons and holes and results in detectors with no capability to resolve radiation peaks.

ACKNOWLEDGEMENT

REFERENCES

1. Proceedings of the Second International Symposium on Cadmium Telluride: Physical Properties and Applications, Strasbourg (1976)
2. Proceedings of SPIE on "Hard X-ray, Gamma-Ray, and Neutron Detector Physics," Vol. 3768, (1999)
3. M. Chu, S. Terterian, D. Ting, C.C. Wang, H.K. Gurgenian, and S. Mesropian, Appl. Phys. Lett. 79, 2728 (2001).

4. A conclusion of discussions between M. Chu from Fermionics Corporation and a group of scientists from Santa Barbara Research Center (currently Raytheon Infrared Operations) led by C.Y. Hwang, 1992.
5. A.G. Thompson, J. Electron. Mater. 2, 47 (1973)
6. M. Fiederle, C. Eiche, M. Salk, R. Schwarz, K.W. Bens, W. Stadler, D.M. Hofmann, and B.K. Meyer, J. Appl. Phys. 84, 6689 (1998)

5.0 UNIFORMITY AND REPRODUCIBILITY OF CdZnTe RADIATION DETECTORS

1. M. Chu, S. Terterian, D. Ting, C.C. Wang, M. Szawlowski, and G.J. Visser, "Uniformity and Reproducibility of CdZnTe Radiation Detectors," IEEE NSS/MIC Conference, Norfolk, 2002.
2. S. Terterian, M. Chu, D. Ting, C.C. Wang, M. Szawlowski, G.J. Visser, and Paul Luke, "Uniformity and Reproducibility of CdZnTe Radiation Detectors," J. of Electron Mater, 32, 796 (2003).
3. S. Terterian, M. Chu, D. Ting, C.C. Wang, M. Szawlowski, G.J. Visser, and Paul Luke, "Uniformity and Reproducibility of CdZnTe Radiation Detectors," The 2002 U.S. Workshop on the Physics and Chemistry of II-VI Materials, San Diego.

Uniformity and Reproducibility Studies of Low-Pressure-Grown Cd$_{0.90}$Zn$_{0.10}$Te Crystalline Materials for Radiation Detectors

S. TERTERIAN,[1,5] M. CHU,[1] D. TING,[1] L.C. WU,[1] C.C. WANG,[1] M. SZAWLOWSKI,[2] G. VISSER,[3] and P.N. LUKE[4]

1.—Fermionics Corporation, Simi Valley, CA. 2.—Advanced Photonix, Inc., Camarillo, CA. 3.—Nova R&D Inc., Riverside, CA. 4.—Lawrence Berkeley Laboratory, Berkeley, CA. 5.—E-mail: sav15@ii.net

A large number of room-temperature detectors have been produced from CdZnTe crystals grown with 10% Zn and 1.5% excess tellurium by the low-pressure, vertical-Bridgman technique. Radiation spectra obtained by these crystals using a ^{241}Am source reveal the characteristic 59.5-keV line as well as the six low-energy peaks, which include the Cd and Te escape peaks. Similarly, ^{57}Co spectra obtained also show a very well-defined 122-keV peak with a 3.1 peak-to-valley ratio. Seven CdZnTe crystals have been grown for reproducibility studies. Four of these crystals have resistivities over 1E9 them. Considering that the indium-doping level is on the order of 2E15 cm^{-3}, the reproducibility is excellent. The theoretical basis of the high-resistivity phenomenon in CdZnTe is discussed in reference to a previous paper. The uniformity of these 6-in.-long CdZnTe crystals is studied, and various measurements are carried out, both laterally and vertically, along the boule. It is determined that, in general, roughly a 3.5-in. section near the middle of the 6-in. boule has sufficient resistivity for producing radiation detectors. This nonuniformity along the vertical direction is caused mostly by the composition change of Cd, Zn, Te, and In-doping level in the growth melt caused by differences in the segregation coefficients of these elements. Although variations in resistivity are seen across some of the wafer slices, most show very good uniformity with high breakdown voltage. Some of the variations are attributed to the different grains within the boule. Similar results are seen in the measured radiation spectra obtain on 4 mm × 4 mm × 2 mm samples from different locations across the wafer, where some samples show well-resolved secondary peaks, while others display only the primary spectral lines.

Key words: CdZnTe, Bridgman growth, gamma-ray detectors

INTRODUCTION

For many applications, such as remote sensing, where detector systems cannot be regularly maintained, it has become increasingly important to produce gamma-ray detectors that require virtually no cooling. The CdZnTe materials have been shown to be a viable alternative to liquid-nitrogen-cooled Ge as well as NaI and HgI detectors for certain gamma-ray applications. Its high z value coupled with a greater efficiency makes it a better choice for small size systems that require good resolution. Throughout the years, different methods have been used to grow

CdTe-based crystals. Although the low-pressure, vertical-Bridgman growth method had been used very early on, it has been replaced by a high-pressure version as the primary method in the last decade. Better understanding of the material properties and origin of electrical properties, a key to producing high-quality crystals for detector applications, has prompted a revival of the earlier growth process. In this paper, the viability of the low-pressure vertical-Bridgman technique is demonstrated with emphasis on uniformity and reproducibility.

EXPERIMENTAL

Seven CdZnTe boules with 10% zinc were grown using a low-pressure, vertical-Bridgman technique.

Excess tellurium was also introduced in the amount
of 1.5% to provide Te-rich conditions, as well as a
small amount of indium doping. The purpose of the
excess Te and In doping is discussed in the next sec-
tion. The crystals were cut along the diameter and
screened for high resistivity and conductivity type.
The conductivity type was determined by separately
applying gold and indium metallization on the crys-
tals and seeing which of the contacts had the least
resistance. The resistivity was determined from re-
sistance measurements taken from a current-voltage
test station at low and high voltages. Once the wafers
were polished, they were subsequently diced into
4 mm × 4 mm squares with a nominal thickness of
2 mm. Straightforward passivation was carried out
using a hydrogen-peroxide solution at room tempera-
ture. The resistivity of the individual detectors was
used for the wafer-mapping data. Once the fabrication
was completed, radiation spectra were obtained using
²⁴¹Am and ⁵⁷Co sources. The spectrum was obtained
on a DSA-1000 DSP system from Canberra Industries
(Meriden, CT). Fourier-transform infrared (FTIR)
measurements as well as infrared (IR) imaging were
carried out to determine bulk properties as well.

RESULTS AND DISCUSSION

Origin of High Resistivity

In an earlier paper, Chu et al.[1] suggested that the
deep-donor level responsible for the high-resistivity
phenomenon in CdZnTe is none other than doubly
ionized Te antisites (Te atoms in Cd sites). Based on
this model, the conduction type of CdZnTe crystals is
determined by the resulting compensation between
the shallow donors of Te antisites and the shallow
acceptors of Cd vacancies, as shown in Fig. 1. High-
resistivity CdZnTe crystals are then produced by
compensating the p-type crystals with indium impu-
rity at a low doping of 1.5 × 10¹⁵ cm⁻³. Using this
model and a better understanding of the defects in
CdZnTe, the crystals were grown under excess Te
with a low amount of indium to provide the low
n-type concentration necessary for high resistivity.

Reproducibility

Table I lists seven crystals that were grown
using the same doping levels and similar growth con-
ditions. All of the crystals showed n-type character-
istics as determined by the method described pre-
viously. Four of the crystals showed resistivities on
the order of 10⁹ Ω-cm or greater. While another two
exhibited lower resistivity of mid-to-low 10⁸ Ω-cm.
However, another crystal showed much poorer

CONDUCTION BAND

— In   — Te_Cd²⁺

                     — Te_Cd⁺⁺

                     — V_Cd⁻
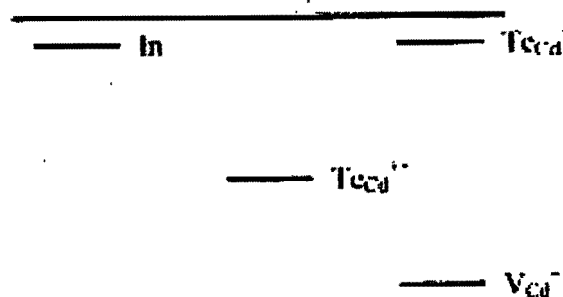
VALENCE BAND

Fig. 1 The proposed deep-level defect model.[1]

electrical properties and was not characterized in
detail. Because four out of seven crystal boules
showed high resistivity, it demonstrates very good
reproducibility considering the low amount of dop-
ing present to compensate for the net concentration
of Cd vacancies, Te antisites, and other impurities.

Uniformity Measurement

Along the Vertical Direction

Resistivity measurements along the length of the
boule show consistently low values at both ends. The
center part tends to exhibit the highest resistivity
values and the greatest uniformity. The measure-
ments also show three semidistinct regions along the
vertical length of the boule. Figure 2 illustrates this
result with semidistinct regions labeled as top, mid-
dle, and bottom. Because of the high segregation coef-
ficient of zinc in CdTe, the bottom region has more
zinc and is more p-type than the middle region. Ear-
lier experiments have shown that the addition of zinc
in CdTe results in a change in electrical property
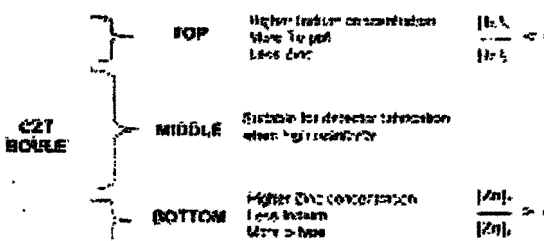
Fig. 2. The illustration of semidistinct regions of CdZnTe crystal.

		Table I. Reproducibility of Crystal Growth among the Similar Doping Runs					
CdZnTe Crystal Number	9564	9571	9572	9898	9988	9989	10131
In doping	2.5E15	2.5E15	2.5E15	2.5E15	2.5E15	2.5E15	2.5E15
Nominal resistivity	1 × 10⁹	5 × 10⁸	2 × 10⁹	4 × 10⁷	5 × 10⁸	4 × 10⁸	2 × 10⁹

Table II. Effect of Zinc Concentration on Conduction Type

X (Zn Contents)	0.0	0.04	0.07	0.10
Conduction type	N	N	N or P	P
Carrier concentration at room temperature (cm^{-3})	1–3 × 10^{15}	2–4 × 10^{14}	.	4–6 × 10^{11}

from n type to p type as seen in Table II, under 1.1% excess-Te conditions. Here, it can be seen that the CdTe crystal (i.e., no zinc) displays n-type behavior with low carrier concentration. As the amount of Zn is added, the crystal becomes increasingly more p type until a high carrier concentration is achieved. This is due, in part, from the decrease in the lattice constant with the increase in zinc concentration and, as a result, a possible decrease in the density of Te antisites, which would then cause the material to be more p type. The FTIR transmission was also carried out to illustrate the decrease in the Zn concentration along the vertical direction of the boule, as shown in Fig. 3. Here, the energy gap is extracted from the cutoff wavelength of the FTIR transmission and clearly shows a decrease in the bandgap along the vertical direction. This can be interpreted as a decrease in Zn concentration because the bandgap of ZnTe is greater than that of CdTe. The top section is affected by a number of characteristic phenomena. First, because the segregation coefficient of indium in CdZnTe is less than one, its concentration tends to increase rapidly in the bulk near the end of the growth. This effect is shown in Fig. 4, where the indium concentration is
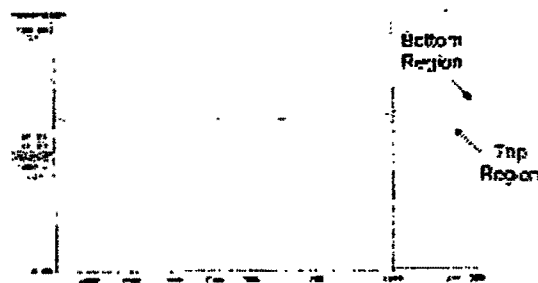
Fig. 5. The FTIR transmission of the two regions of the crystal.

plotted versus the amount solidified for different segregation coefficients. The relation used, which assumes complete homogeneity, is given by

$$C_s = k_0 C_0 (1 - X)^{k_0 - 1}$$

where X is the fraction of liquid solidified, k_0 is the segregation coefficient, C_s is the concentration in solid, and C_0 is the initial impurity concentration in liquid.

A segregation coefficient of 0.35 is used for the doping calculations for the crystal growth. It can be seen that the indium concentration increases by roughly a factor of about 2.5 in the middle area of the crystal and increases rapidly near the end, which is the effect of a low-segregation coefficient. This increase in the middle region is not very large considering the doping level within the CdZnTe crystal, but nonetheless, it is still there. Second, the number of Te precipitates increases near the end of the growth, and as a result, the percent of transmission decreases, as shown in Fig. 5. Because we have been routinely using transmission measurements for thousands of substrates for IR detectors over the years, this method is very reliable after chemically polishing a fair amount of material. Although it does not quantify the level of Te precipitates, it does give a clear indication of the relative amounts. This increase in the inclusion of the Te precipitates has the effect of increasing the p-type concentration. As stated earlier, the zinc concentration has also decreased in this region but cannot compensate for the detrimental effect of the large quantity of Te precipitates.

Along the Horizontal Direction

The situation across the sliced wafer, however, is much more uniform, as shown in Figs. 6–8, for the three different crystals. Here, the grids on the crystals indicate the individual detectors that are diced, and the shaded devices are among the ones tested. It can be seen that on these characterized wafers,

Wafer slice	Energy Gap	
Top-1	Eg = 1.493 eV	
Top-2	Eg = 1.499 eV	
Bottom-2	Eg = 1.508 eV	
Bottom-1	Eg = 1.515 eV	
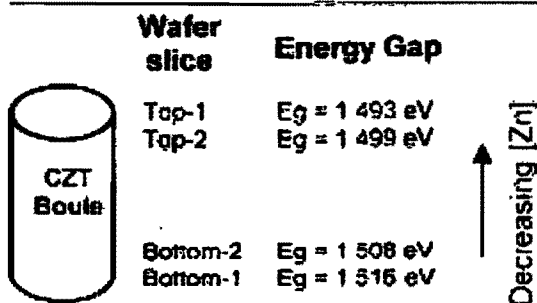
Fig. 3. The decreasing energy gap of different wafer slices reflecting the decrease in concentration of zinc along the vertical length of the boule.
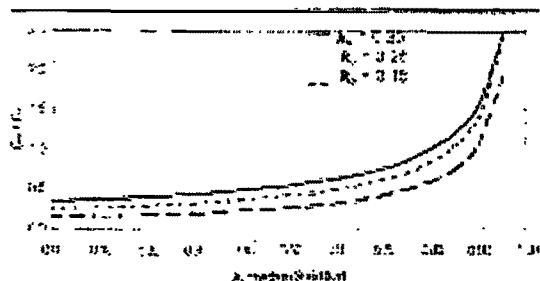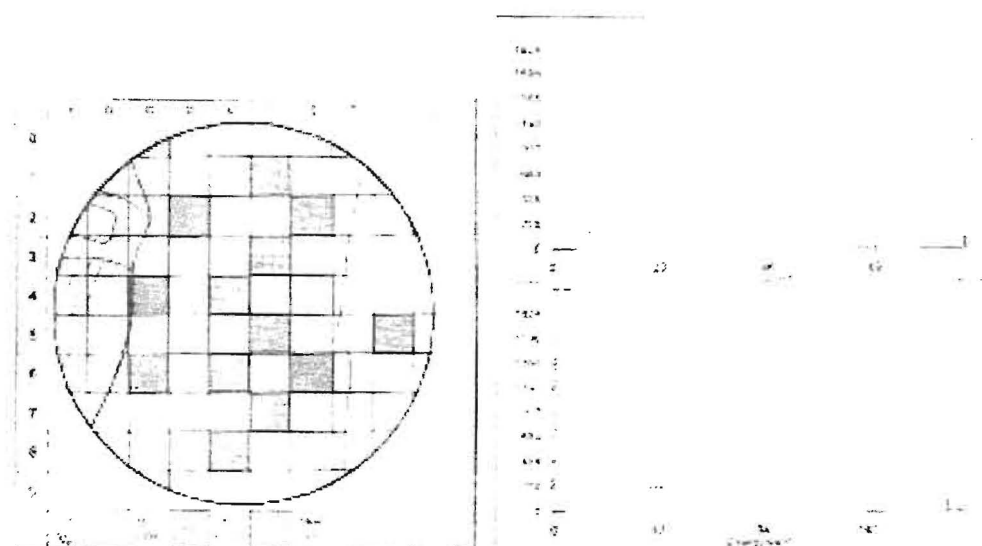

Fig. 4. The In-segregation coefficient in CdZnTe.

Fig 6 The uniformity map and ^{241}Am and ^{57}Co spectrum obtained from Cd$_{0.9}$Zn$_{0.1}$Te crystal 9571
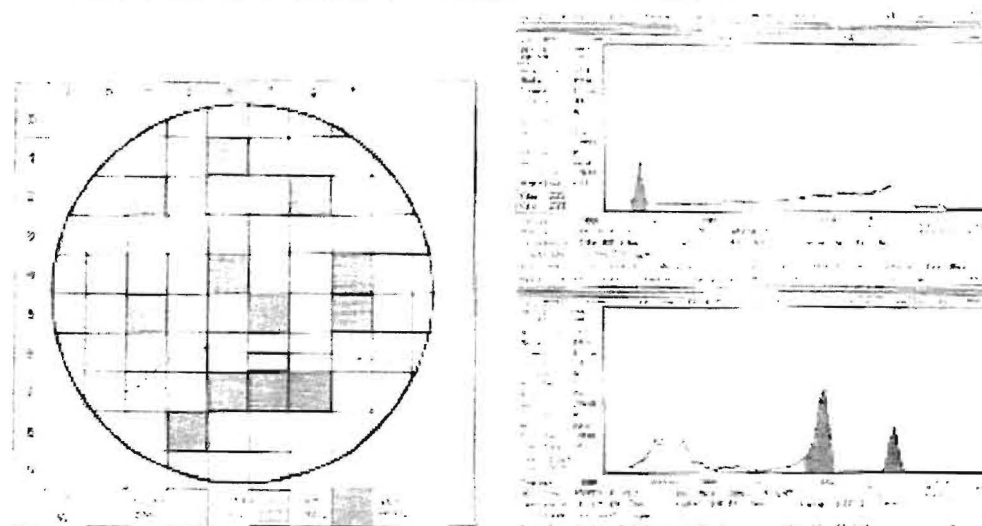

Fig 7 The uniformity map and ^{241}Am and ^{57}Co spectrum obtained from Cd$_{0.9}$Zn$_{0.1}$Te crystal 9571

the resistivity is consistent and within less than
an order of magnitude from die to die. On the
good wafer samples, the resistivity is greater than
10^{10} Ω·cm. Some of the variation among the dies is
breakdown voltage, where some samples show a

breakdown of only 200–300 V, while other dies ex-
hibit breakdown voltage much greater than 600 V
and over 1,000 V. The breakdown voltage was de-
fined as any sudden increase in the dark current
above 5 μAmps. This variation could be related to
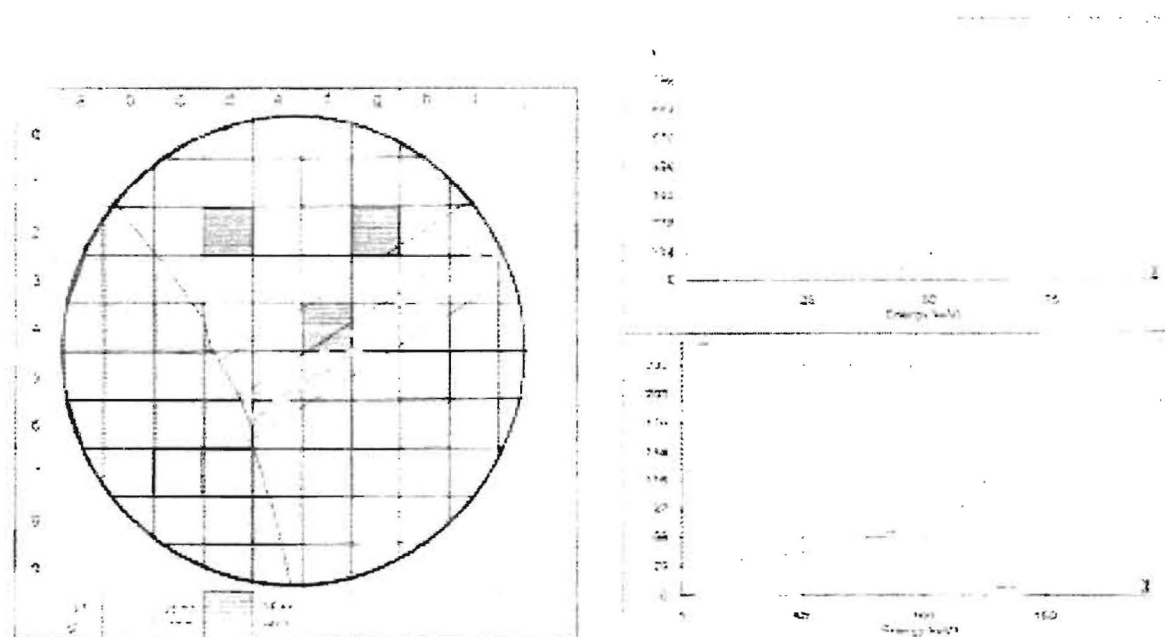
Fig. 8. The uniformity map and ^{241}Am and ^{57}Co spectrum obtained from $Cd_{0.9}Zn_{0.1}Te$ crystal 9989.

surface conditions because the surface passivation was not optimized. On the other hand, the bulk properties can also affect the surface state and, ultimately, the surface passivation.

The spectra obtained from these diced samples reveal the effect of the resistivity on performance, where dies with resistivities on order of 1E9 Ω-cm and greater show good spectral resolution at room temperature, as shown in Figs. 6 and 7 for the two different crystals. The Cd and Te escape peaks as well as the characteristic low-energy peak of the ^{241}Am is clearly revealed from these detectors with resistivities greater than 1E9 Ω-cm. However, these close peaks are convoluted for devices with resistivity values that are less than ~4E8 Ω-cm as shown in Fig. 8 for the other crystal. These results are consistent among many samples tested. Similarly, the ^{57}Co data show higher resolution of the 122-keV peak for devices that are greater than 10^9 Ω-cm. It is unclear where the threshold for good spectra lies; however, the results indicate that dies grown under similar conditions with resistivities greater than 10^8 Ω-cm and with a breakdown voltage greater than 600 V will most likely yield better detectors.

It is also evident that the different grains do not always result in different performance characteristics, as illustrated from the previously mentioned figures. For example, crystal 9872 and 9989 exhibit identical performance for dies from different grains. Yet, crystal 9871 shows some difference in resistivity between the two grains. However, more data must be extracted from these experiments to fully understand and make any concrete predictions on this correlation.

Bulk Properties

Figures 9 and 10 show signal-intensity maps within a single detector, where a ^{57}Co spot source was used to incrementally map the device every 0.5 mm. The outer edges behave as infinite-trap centers, and as expected, exhibit poor performance and, thus, have a low number of counts at the 122-keV energy peak. The center and outer areas of the detector in Fig. 9 show very good uniformity. While the detector shown in Fig. 10 displays nonuniform characteristics near a corner of the outer region. This can be due to some Te precipitates within the detector, as shown in an IR image of a wafer slice in Fig. 11. The small dark spot on the wafer illustrates the likelihood of a

Fermionics Ralph#0
sample
5x5x3 mm
file 010601
200 gain
100 Volt
2 microsec shaping
120 sec/step
0.5 mm stepsize
Co57
el Au contacts.
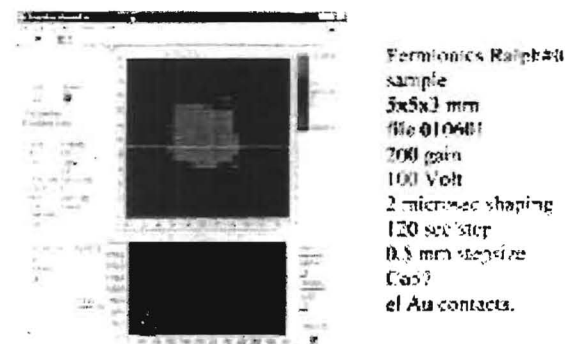
Fig. 9. The spectral-intensity map within a detector area.

Te precipitates, which can be confined within a detector area.

Larger detectors with a size of 10 mm × 10 mm × 12 mm were processed to obtain additional uniformity data. Figure 12a shows the IR transmission of a sample taken from another crystal grown under conditions similar to the other seven crystals but sliced into thicker wafers. Although there are some Te precipitates on the order of about 5–10 μm, the image does not show any presence of very large precipitates. The dark regions on the edges are due to saw damage. This detector was tested to have 3.5 × 10¹⁰ Ω-cm and was biased to 1,000 V. Figure 12b shows the 5-MeV alpha-particle spectrum of ²⁴¹Am incident on this device. While it does not exhibit excellent performance with a resolution of about 5%, it

reflects a decent uniformity of the bulk material that can be used for certain applications.

SUMMARY

Of the seven crystals that were grown with similar parameters, four exhibited very high resistivity and good detector performance at room temperature. These four crystals had resistivity values on the order of 10¹⁰ Ω-cm. While another two showed marginal characteristics of resistivity and performance, and the remaining one exhibited poor characteristics. It should be noted that the amount of indium doping is on the order of 0.1 ppm in the crystal. Therefore
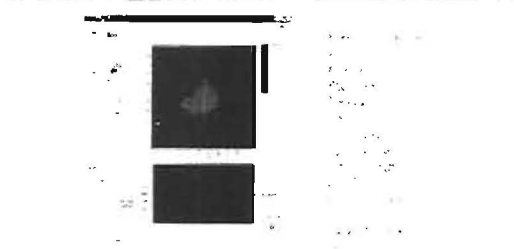
Fig. 10. The spectral intensity map within a detector area.
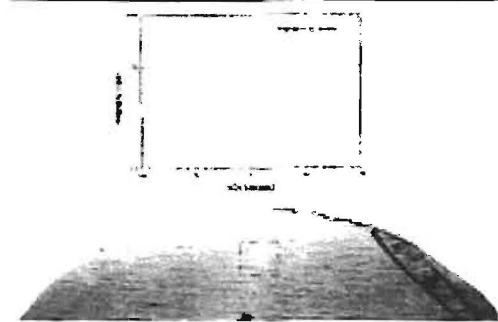
Fig. 11. The IR image of wafer showing Te precipitates

Sample size: 10.4mm × 10.75mm × 12.5mm

Bulk resistivity: ρ = 3.5×10¹⁰ Ω·cm

Infrared transmission image of the crystal when illuminated from the BOTTOM and viewed from the TOP.

a
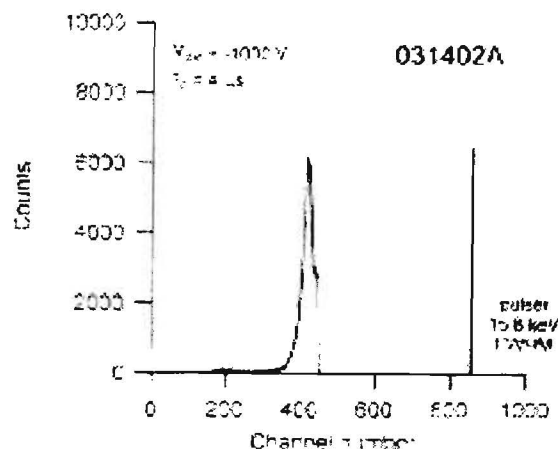
²⁴¹Am 5.5 MeV alpha-particle spectrum obtained with the planar detector at a field of about 1000V/cm. The alpha particles were incident on the BOTTOM electrode

b

Fig. 12. (a) An IR image and (b) alpha-particle spectrum of 10 mm × 10 mm × 12 mm detector.

28

the reproducibility is excellent considering that this low amount of doping compensates the net Cd vacancy and Te antisites as well as all the other defects within the material. Also, the two crystals showed a nominal resistivity of $\sim 2 \times 10^6$ Ω-cm, which is not very far from the desired 10^9 value, which seems necessary for good device performance.

The uniformity across the vertical and horizontal direction is largely due to the segregation coefficients of indium and zinc. Although Te precipitates are prevalent throughout the crystal, they are mostly concentrated near the top end of the boule, which affects the crystal properties in a number of way, including lower transmission, increase in p-type concentration, and increase in trap centers. The bottom part of the boule, which is the initial region of crystallization, has smaller grains and a high amount of zinc that will make the material more p type as compared to the center region and, as a result, will tend to have a lower resistivity. As a result, about two thirds of the crystal near the middle part of the boule can be used for device fabrication with the optimum electrical and crystalline properties. The situation along the horizontal

length of the boule is more uniform in terms of the resistivity values seen in dies within a wafer slice, and most exhibit a small amount of variation, typically by less than a factor of 2. In many instances, the variation is in the breakdown voltage, which for most devices is much greater than 600 V, while for others it is only about 200–300 V. This could be due to the compositional and defect variations in the bulk, or perhaps anomalies at the surface, such as surface-recombination centers caused by poor passivation. A detailed study and detector-wafer mapping of additional crystal slices can shed more light on the uniformity of the crystals and the variations seen within the boule.

ACKNOWLEDGEMENTS

REFERENCE

1. M. Chu, S. Teterman, D. Ting, C.C. Wang, S. Gurgenian, and S. Mesropian, Appl. Phys. Lett. 79, 2728 (2001).

6.0 DISTRIBUTION OF THE HIGH RESISITIVITY REGION IN CdZnTe AND ITS EFFECTS ON GAMMA-RAY DETECTOR PERFORMANCE

1. Sevag Terterian, Muren Chu, and David Ting, "Zn Distribution in CdZnTe and its Effects on Detector Performance," SPIE Meetings, San Diego, 2003.
2. S. Terterian, M. Chu, and D. Ting, "Distribution of the High Resistivity Region in CdZnTe and its Effects on Gamma-ray Detector Performance," The 2003 U.S. Workshop on the Physics and Chemistry of II-VI Materials, New Orleans.
3. S. Terterian, M. Chu, and D. Ting, "Distribution of the High Resistivity Region in CdZnTe and its Effects on Gamma-ray Detector Performance," Submitted to J. Electron. Mater.

Distribution of the High Resistivity Region in CdZnTe and its Effects on Gamma-ray Detector Performance

S. Terterian, M. Chu, and D. Ting

Fermionics Corporation, Simi Valley, CA

ABSTRACT

The effect of the location of the high resistivity region on gamma-ray detector performance within the crystal boule is investigated for 10% zinc with 1.5% excess Te. By varying the indium doping concentration in several CdZnTe boules, the region of high resistivity is seen to move along the vertical length of the crystal. The variation of the zinc concentration within the crystal boule is compared with the location of the high resistivity region along the length of the crystals. The concentration of zinc is extracted from FTIR measurements, and the segregation coefficient is calculated using data obtained from the CdZnTe crystals. The zinc distribution is plotted in terms of the location along the crystal length in order to correlate the concentration with detector performance. Radiation spectra obtained from the 122KeV gamma rays using a ^{57}Co source reveal a strong dependence between detector performance, and the relative location of the high resistivity region within the crystal. Initial results suggest that there are three semi-distinct regions along the length of the boule that give very different characteristics, where it can be said that the best detector performance is in the middle region with a 6 % resolution of the 122KeV peak, which is quite good for test detectors without a guard ring such as these. It is determined that this middle region has a zinc concentration of ~9-11%, which varies slightly from the original concentration of 10%. The differences in the performance characteristics is discussed, and defect distribution within the crystal as the main source of the variation is suggested. Also, based on the results, it is believed that the role of indium is essentially to compensate the vacancies in the crystal, and therefore, secondary to the crystalline properties and impurities within the boule. Overall, it is believed that crystalline defects and inclusions play a greater role in determining the performance characteristics of CdZnTe radiation detectors.

Keywords: CdZnTe, Bridgman Growth, Single Crystal, Gamma Ray Detectors

1. INTRODUCTION

Over the recent years, increasing interest in the area of un-cooled gamma-ray radiation detectors has occurred. Most recently, a serious need is seen in sensitive, low cost, and portable detectors for homeland security. Although CdZnTe is a prime candidate that possesses most of the qualities sought today, it has fallen short of expectations due to poor yield emanating in part from defects and trap centers, especially for medium energies as the 122KeV peak of a ^{57}Co source. Therefore, in order to obtain higher yields, it has become necessary to better understand the chemistry involved in the crystallization of CdZnTe, especially with the distribution of the native constituents. For gamma-ray detector applications, it is important to obtain crystals with high resistivity, such that the Fermi level can be pinned near the middle of the band gap, and thus, a high bias can be achieved before breakdown occurs. This would make it easier for the photo-generated electron-hole pairs to be collected in the high electric field due to the high bias. In this paper, we set out to investigate the effect of the high resistivity region at different locations within the crystal boule in order to obtain a greater understanding of the behavior of the various types of defects.

2. EXPERIMENTAL

Several CdZnTe crystals were grown with 10% zinc concentration by low pressure vertical Bridgman technique. In order to properly determine the effect of zinc concentration on device performance for a given starting concentration of 10%, the location of the high resistivity region was changed by varying the amounts of indium in the boule for different runs. This has the effect of changing the location of the high resistivity region within the boule, while the starting zinc concentration is kept constant from run to run, so that the net effect is to obtain a variation only of the zinc concentration along the length of the boule.

Once the wafers were sliced, they were chemically polished using a Br-HBr- Ethylene Glycol solution. The zinc concentration was determined by first measuring the cut-on wavelength of the CdZnTe wafers using a Perkin-Elmer FT- NIR Spectrometer. The data was then inserted in the following equation from Hirano[1], which was derived from ICP techniques and verified by NIR experiments;

$$Zn(\%) = 289.36 - 0.33804 \ \lambda(\alpha) \qquad (1)$$

The term, $\lambda(\alpha)$, is defined by the wavelength corresponding to an absorption coefficient of $\alpha=10\text{cm}^{-1}$. We have found that a better fit exists when the 50% cut-on value is used for the wavelength when covering a greater span of Zn concentration, although, they are both very close. This data set is then used to extract the segregation coefficient and the initial concentration using first order mass balance equations.

The resistivity was determined from resistance measurements taken from a I-V test station at low and high voltages. Once the wafers were polished, they were subsequently diced into 4mm by 4mm squares with a nominal thickness of 3mm. A simplified passivation technique was carried out using hydrogen peroxide solution at room temperature. No guard rings were applied to these devices. Once the fabrication was completed, radiation spectra were obtained using ^{57}Co sources at room temperature. The spectrum was obtained on a DSA-1000 DSP using Genie 2000 software system from Canberra Industries, along with corresponding pre-amplifier.

3. RESULTS AND DISCUSSIONS

Zinc Distribution

The FTIR curves are shown in Figure 1 for different slices along a CdZnTe boule, as well as a FTIR curve of a CdTe wafer. The energy gap was extracted from the cut-on wavelength corresponding to the 50% transmission. This method provided the most accurate results as it gave the best fit when a reference CdTe wafer was used which has a known band gap of 1.446 eV. Table 1 lists the zinc concentration calculated from the equation above. It can be seen that the bottom region, which is first to solidify, has a higher concentration than that of the top final region that solidifies. This is because, since the segregation coefficient for zinc is positive, there will be a tendency for the newly solidified portion to be higher in zinc concentration than the final solidified region.

The segregation coefficient can be extracted from the following equation, which assumes complete mixing;

$$C_s(x) = kC_0 \left(\frac{l-x}{l}\right)^{k-1} \qquad (2)$$

Where, $C_s(x)$ is the concentration in the solid and C_0 is the initial Zn concentration in the melt, l is the length of the crystal, x is the fraction solidified, and k is the segregation coefficient. Entering the data from Table 1 into the equation above gives a range in segregation coefficient between $K = 1.25$-1.42. This range in value is very close that reported earlier by Fougeres[2], which had obtained a segregation coefficient of k=1.30 for best fit. It is also in the range of 1.05- 1.60 cited by Radhakrishnan[3]. Table 2 lists the zinc segregation coefficient from various sources. Figure 2 shows a plot of Equation 2 for the different k values that were obtained in this experiment. The dashed line corresponds to a segregation coefficient of 1.34, which fits the data somewhat better as it is near the middle of the calculated coefficient range. Since zinc has a greater tendency to go into the solid phase than cadmium, the initial ratio in the solid is higher than that in the initial solution. The concentration then tends to decrease as the fraction solidified increases. It can be seen that the concentration rolls off to nearly 4% at the end of the growth. When an initial concentration, C_0, of 9.5% is used, the fit is much better, as can be seen in Figure 3. This could be due to the post growth solid-state diffusion that takes place at the relatively high temperatures after the growth.

High Resistivity Adjustment and ^{57}Co Spectra

In an earlier paper[4], the concentration of indium in CdZnTe was shown to increase as the growth progressed due to a segregation coefficient that is less than one in this material. The role of indium is essentially to

compensate for the net cadmium vacancies and tellurium anti-sites. As a result, by changing the starting indium concentration, the location of the high resistivity region within the CdZnTe boule can be changed. In the case of these crystals, the indium concentration was varied from $1x10^{15}$ – $5x10^{15}$ cm^{-3} to change location of the high resistivity region from the lower end all the way to the top of the crystal. For these crystals, the high resistivity regions were on the order of $5x10^9$ Ω-cm - $2x10^{10}$ Ω-cm.

For the purpose of clarity, we have divided the crystal boule into three semi-distinct regions as shown in Figure 4. A typical ^{57}Co spectrum obtained from the lower section of crystal that was optimized is shown in Figure 5. While figure 6 shows the spectrum of the middle part of another crystal that was optimized for high resistivity. Finally, the spectrum obtained from the top region of a crystal optimized for resistivity is shown in Figure 7. The detectors produced from the crystal with the lower end optimized for high resistivity shows a very poor 122KeV peak which is barely noticeable. From the above experiments for the zinc distribution, we know that there is a high concentration at the lower end of the crystal. We have also shown in an earlier paper, that a high concentration of zinc tends to produce poorer detector performance. This is believed to be the result of too few tellurium anti-sites in the region brought on by the reduction of the lattice constant and the subsequent increase in the formation energy of the Te-anti-site. As a result, there exists a greater number of cadmium vacancies which act as effective trap centers, and ultimately yield poor detector performance, especially with that of higher energy radiation.

For detector performance in the crystals with the top region optimized for high resistivity, it can be seen that in Figure 7 hardly any peak exists for the 122 KeV energy of ^{57}Co source. Although, the zinc content is a few percent lower than the starting concentration, it may have a smaller effect on detector performance when other bulk properties are carefully considered. Table 3 shows data from an earlier paper[5] which describes the results of adding increasing amounts of excess Te in the crystal, where it can be seen that a greater amount of excess Te results in poor resolution of small secondary peaks as well as high energy peaks. Too much excess Te will also result in large tellurium precipitates as well as inclusions, which also act as very effective trap centers for electrons and holes within the crystal, and result in poor signal collection for the device. CdZnTe wafer slices taken from this top region will tend to have lower IR transmission due to these tellurium precipitates, which absorb energies in the far infrared. This lower transmission is obvious in Figure 1 for the top region.

In the case of the crystals with the middle region being optimized for high resistivity, we can see that the ^{57}Co spectrum is quite good as shown in Figure 5, where the 122KeV peak shows a resolution of about 5% at room temperature. The zinc concentration in this middle part of the crystal boule is in the range between 8.5% to 11.5%, with the center being very close to the starting concentration of 10%. The lower part of the middle region seems to be the optimum, with a zinc concentration of about 11%.

4. SUMMARY

The variation of the zinc concentration within the CdZnTe crystal boules was compared with the location of the high resistivity region along the length of the crystals with a starting zinc concentration of 10% and 1.5% excess Te. By varying the indium doping concentration in several CdZnTe boules, the region of high resistivity is seen to move along the vertical length of the crystal. The effect of the location of the high resistivity region within the crystal boule was investigated. The concentration of zinc was extracted from FTIR measurements, and the segregation coefficient calculated using data obtained from the CdZnTe crystals. The zinc distribution was then plotted in terms of the location along the crystal length in order to correlate the concentration with detector performance.

Results suggest that there are three semi-distinct regions along the length of the boule that give very different characteristics, where it can be said that the best detector performance is in the middle region, especially at the lower part of the middle region with a 6% resolution. It is determined that this middle region has a zinc concentration of ~9-11%, which varies slightly from the original concentration of 10%. Although, the resistivity was optimized in the other regions to obtain high breakdown voltage for spectrum analysis and proper detector performance, the inherent crystal quality was unchanged. From the results, it is very likely that crystalline defects and inclusions play a greater role in determining the performance characteristics of CdZnTe radiation detectors, perhaps more so than the amount of zinc. Because the amount of indium used to dope the material and obtain high resistivity crystals is very low (mid 10^{15}), it is unlikely that impurities have played a large role in the performance

of these gamma-ray detectors. However, more tests should be carried out to verify this assertion. Nevertheless, additional work is necessary to adjust the zinc concentration so that the middle part of the crystal, where it is believed that crystalline imperfections are minimal, has differing amounts of zinc for different boules, in order to determine whether an ideal concentration exists.

REFERENCES

[1] R. Hirano, A. Hichiwa, H. Maeda, and T. Yamamoto, *Journal of Electronic Materials*, Vol. 29, No. 6, 2000.
[2] P. Fougeres, et. all, Journal of Crystal Growth, Vol. 197 (1999), 641-645.
[3] J.K. Radhakrishnan, et. all, *Bull. Material Science*, Vol. 24, No. 6, 2001. 659-663.
[4] S. Terterian, M. Chu, D. Ting, L.C. Wu, C.C. Wang, M. Szawlowski, G. Vissor, and P.N. Luke, Journal of Electronic Materials, Vol. 32, No. 7, 2003.
[5] M. Chu, S. Terterian, D. Ting, C.C. Wang, H. Gurgenian, S. Mesropian, *Applied Physics Letters*, Vol. 79 No. 17 October 2001.
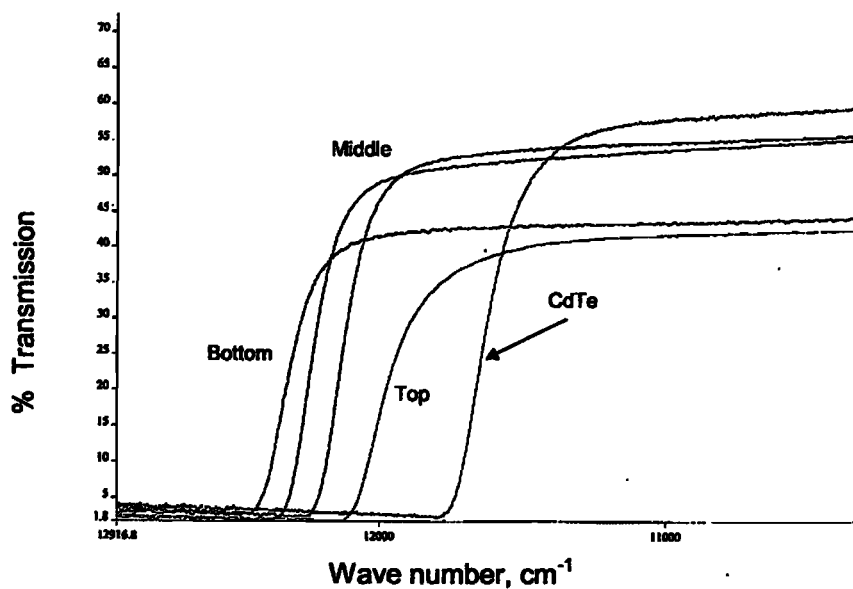
Figure 1. FTIR spectrum of different water slices along a CdZnTe crystal, as well as a CdTe wafer sample.
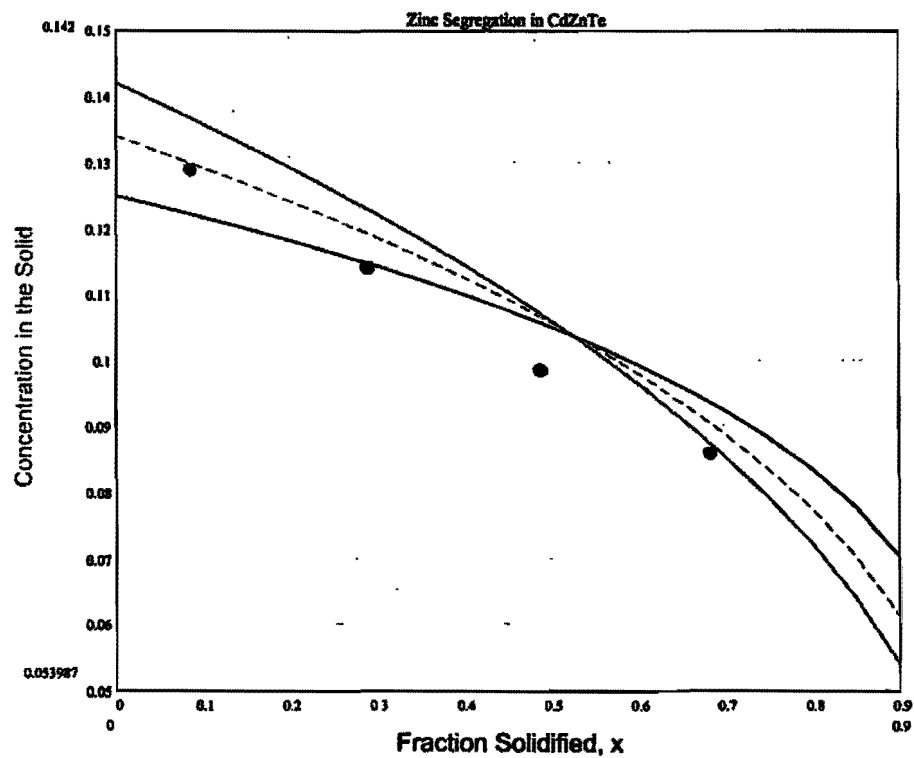
Figure 2. Zinc segregation in CdZnTe crystal.
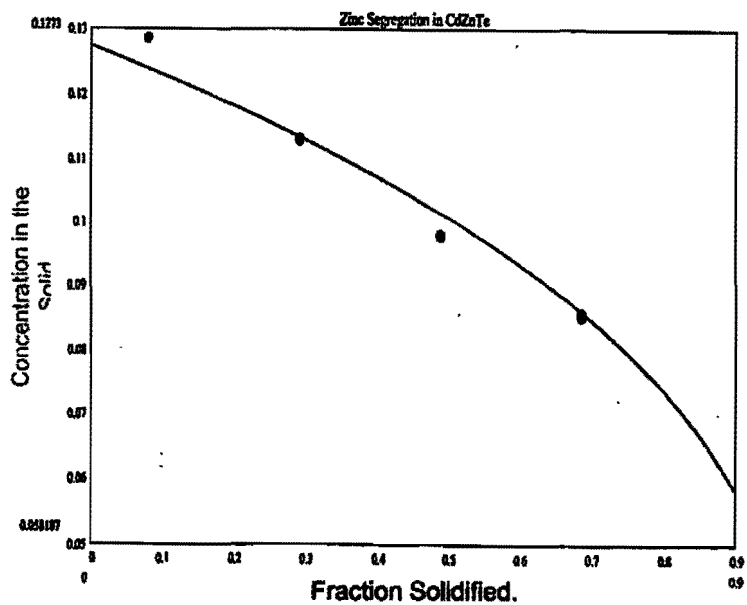
Figure 3. Zinc segregation in CdZnTe crystal.

35
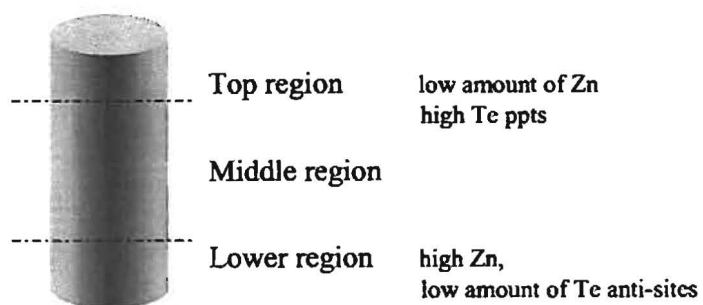
Figure 4. Three semi-distinct regions of CdZnTe.
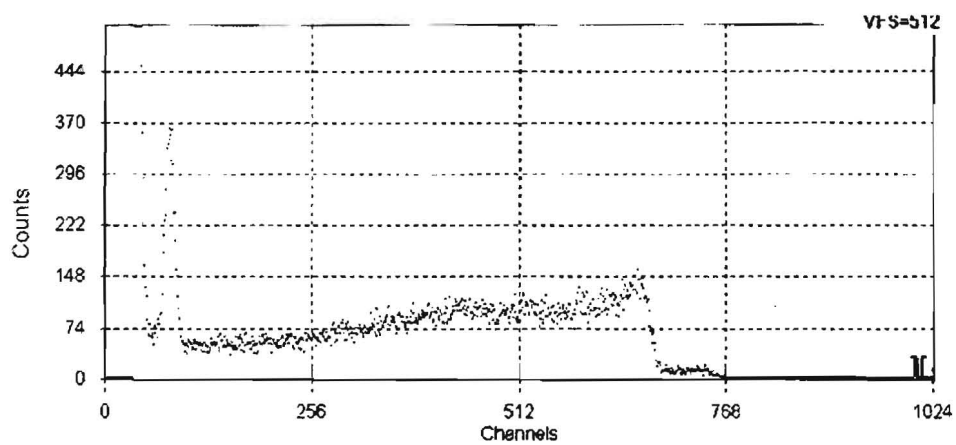
Figure 5. Radiation spectrum obtained from the bottom part of CdZnTe crystal boules.
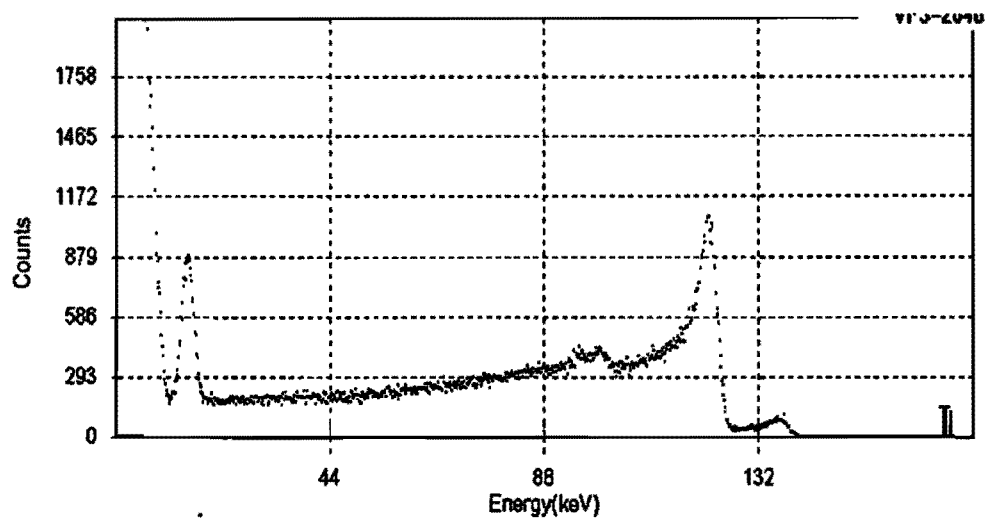
Figure 6. Radiation spectrum obtained from the middle region of a CdZnTe boule.
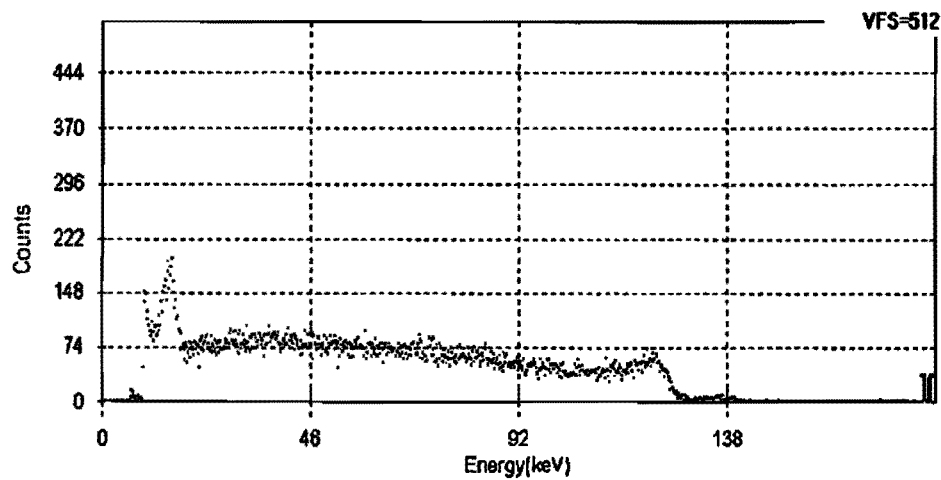
Figure 7. Radiation spectrum obtained from the top region of a CdZnTe boule.

Table 1: Zinc composition extracted from FTIR measurements

Wavelength (nm)	Zn Concentration	Fraction solidified
817.9	12.9%	0.08
822.3	11.3%	0.29
827.2	9.7%	0.49
830.5	8.6%	0.68

Table 2: Zinc segregation coefficient from literature.

source	k
Fougeres	1.30
Radhakrishnan	1.17
Weigel	1.45
Capper (cited in Radhakrishnan)	1.05-1.60

Table 3: Effect of increasing excess Te in the crystal

Stoichiometry (Te/(Cd+Zn))	1.000	1.010	1.015	1.020	1.030
Crystal Log #	9294	9489	9872	9618	9238
Resistivity ($\Omega \cdot cm$)	10^8	10^8	$\geq 10^9$	$\geq 10^9$	$\geq 10^9$
FWHM of ^{241}Am @ 59.5 keV	Not Resolved	Resolved	3.6 keV	6.5 keV	6.6 keV

7.0 ROLE OF ZINC IN CdZnTe RADIATION DETECTORS: WHY ZINC? HOW MUCH?

1. M. Chu, S. Terterian, and D. Ting, "Role of Zn in CZT Radiation Detectors: Why Zinc? How Much?" IEEE NSS/MIC Conference, 2003.
2. M. Chu, S. Terterian, and D. Ting, "Role of Zn in CZT Radiation Detectors: Why Zinc? How Much?" Submitted to IEEE Transaction on NSS/MIC Conference, 2003.

ROLE OF ZINC IN CdZnTe RADIATION DETECTORS: WHY ZINC? HOW MUCH?

Muren Chu, Sevag Terterian, and David Ting

Abstract-CZT crystals with Zn contents of 0%, 10%, 15%, and 20% have been grown and detectors have been produced. Infrared transmission measured on the wafers sliced from these crystals shows that as the Zn content increases, there is a reduction in the transmission toward longer wavelengths, indicating the existence of an increasing amount of larger Te-precipitates. For producing high resistivity materials, a higher concentration of indium is also required for CZT with higher Zn content. The best detectors were produced in CZT with 10% Zn, while CdTe detectors are unable to resolve the ^{57}Co 122keV peak and CZT detectors with 15% and 20% Zn display high noise levels at energies below this peak.

The above results are explained by a model that the role of Zn in CZT is to reduce the density of Te_{Cd}, to increase the density of V_{Cd}, and to enhance the diffusion rate of V_{Cd}. The higher amount of Te-precipitates in CZT with more Zn is caused by the rapid merge of V_{Cd} through fast diffusion of V_{Cd}. Because of the trapping by the Te-precipitates, detectors fabricated on CZT with 10% and 20% Zn are inferior to the 10%Zn CZT detectors. On the other hand, CdTe and CZT with Zn content less than 7% Zn have a high concentration of Te_{Cd}, V_{Cd}, and complexes such as $Te_{Cd} \cdot V_{Cd}$ and $Te_{Cd} \cdot (V_{Cd})$, which are also trapping centers. As a result, the detectors fabricated on these crystals are also inferior to the 10% Zn detectors. The optimal Zn content for CZT grown using our technique is therefore near 10%.

Key Words: CdZnTe, CZT, Radiation Detector, Defect, Cd Vacancy, Te Antisite, Te Precipitate

1.0 INTRODUCTION

CdZnTe (CZT) detectors have been used for many applications in recent years[1] and tremendous efforts have been directed to improving and to understanding CZT materials.[2-7] Two interesting questions arise regarding using CZT instead of CdTe for producing room temperature detectors: (i) how does Zn improve the detector performance, and (ii) what is the optimal Zn content for producing the best detectors? This paper attempts to answer these two questions using a model involving native defects of Cd vacancies (V_{Cd}) and Te antisites (Te_{Cd}, Te at Cd sites). In Section 2, the basic theory of evolvement of V_{Cd} and Te_{Cd} in CZT is presented. Section 3 describes experimentally and theoretically how the evolved defects affect the properties of CZT materials and detectors. Based on the above results and discussion, a model is proposed in Section 4 to answer the above two questions. Finally, the findings of this paper are summarized in Section 5.

2.0 THEORY ON DEFECTS

In References 2 and 6, it was shown that CdTe and CZT grown with 1% or less excess Te using the Bridgman technique have residual Cd left in the growth quartz crucible while the crystals grown with 1.1% or more Te excess have residual Te left. This phenomenon indicates that CdTe/CZT can accommodate 1% or more excess Te at growth temperature. In Reference 2, it was also demonstrated that with 1.1% or more excess Te, the as-grown CZT with a Zn contents less than 7% are p-type. This indicates the crystals have more Te_{Cd} than V_{Cd} at room temperature. But under the identical growth conditions, CZT with Zn contents over 7% are p-type because of more V_{Cd} than Te_{Cd}. At room temperature, the concentration of Te_{Cd} and V_{Cd} are on the order of 10^{15} to 10^{17} cm^{-3}.

Based on thermodynamics, under equilibrium conditions, the concentration of any point defect at any specific temperature can be written as

$$C_i = C_{oi} \cdot \exp(- E_i/kT) \tag{1}$$

Where C_o is partial pressure dependent but temperature independent constant, E_i is also a partial pressure dependent defect formation energy. Using this equation, the dynamics between the defect species and densities at growth temperature and those at room temperature can be described by the following simple model based on

$Cd_{0.9}Zn_{0.1}Te$ grown with more than 1.1% excess Te.[2] As shown in Figure 1(a), V_{Cd} and Te_{Cd} are the dominant defects at CZT growth temperature. Each V_{Cd} is counted as one excess Te atom and Te_{Cd} is counted as two excess Te atoms. The densities of these defects are on the order of 1×10^{20} cm^{-3}. According to Eq. (1), the densities of these defects will be reduced during the post-growth cooling period from growth temperature to room temperature. Since Te_{Cd} is not a mobile species, it is reasonable to assume that the diffusion of V_{Cd}, especially through Zn sites, dominates the process of reducing the densities of both Te_{Cd} and V_{Cd}.

If during the cooling period, the equilibrium condition is not maintained and V_{Cd} is not allowed to diffuse out of the CZT crystals, the resultant defect species will be similar to those shown in Figure 1(b). Some of the V_{Cd} will form defect complexes with Te_{Cd} to form defect complexes such as $Te_{Cd}(V_{Cd})^2$ and $Te_{Cd}(V_{Cd})$.[6] The other V_{Cd} will merge together to form voids with Te precipitates inside. The size of the Te precipitates can vary from sub-microns to tens of microns.

In principle, if the post-growth cooling is kept in equilibrium with the overpressure,[8] The defects can diffuse out of the crystal and their densities will be reduced from Figure 1(a) to Figure 1(c) during the cooling process. However, this process may not be practical, especially at lower temperature because it takes a lengthy duration for the equilibrium to be maintained. The most probable result is shown in Figure 1(d). The densities of point defects are similar to those in Figure 1(b), but the densities of other defects are much less.

Infrared transmission measurement is a powerful tool used to estimate the size and the relative amount of the Te precipitates. Based on basic wave theory, a photon with its wavelength comparable to or smaller than the particle will be scattered. Therefore, from the reduction of infrared transmission, the size and quantity information of the Te precipitates in CZT can be obtained. For this paper, the transmission curves have been measured on 2.5mm thick CZT/CdTe wafers for analysis.

3.0 EXPERIMENTAL RESULTS AND DISCUSSION

CZT Crystal Growth and Device Processing

The 1.5" to 2.2" diameter CZT crystals have been grown by the vertical Bridgman technique. For consistency, all crystals to be discussed in this paper have a diameter of 1.5" and a boule length of 6". For better detector property, 1.5% excess Te have been introduced into the growth melt for defect control.[6] Raw Cd, Te, and Zn in 7N impurity grade are the standard starting material. Occasionally 6N grade materials are used for impurity investigation purpose. But no significant effect has been observed between the 6N and 7N raw materials.

In Reference 9, we reported that the best section of each crystal for producing detectors is the region 30% - 50% from the lower end of each boule. Therefore, all of the detectors produced for this paper are fabricated from this particular section of each crystal.

The CZT detectors with a 4mmx4mmx3mm size have a simple planar structure. Au contacts were deposited onto the opposite sides of the 3mm dimension and oxide was applied for surface passivation. No guard ring was employed.

CdTe Material and Detector

The infrared transmissions at various sections of undoped CdTe grown with 1.5% excess Te have been measured and are shown in Figure 2. The horizontal axis is the wave number, which is equivalent to a wavelength range from 2.2 – 22.0μm. Due to reflection loss, the maximum theoretical transmission is 67%. Curve 1 represents the transmission of CdTe near the bottom of the boule. The fall off in the far infrared region is due to free electron absorption, which indicates the n-type conduction of the as-grown, undoped CdTe. In the 2.2 – 5.0μm region, the transmission is 64%, demonstrating a low density of Te-precipitates in dimensions equivalent to these wavelengths. Curve 2 represents the transmission measured in the CdTe section 20% - 60% from the bottom of the crystal. The smaller fall off in far infrared than that shown in Curve 1 suggests that the electron density in this section of CdTe is less than that in the bottom region. The existence of small Te-precipitates can be visualized from the reduced transmission in the 2.2 – 3.0μm wavelength.

Curve 3 represents the transmission measured in the CdTe section 60% - 85% from the bottom of the crystal. This curve is similar to the one in Curve 2 except that there is no far infrared fall off. However, Hall measurement shows that the material remains n-type. Curve 4 is the transmission measured on wafers sliced from the top 15% of the CdTe crystal. The reduced transmission indicates the existence of Te-precipitates with sizes up to 10μm and beyond. Hall measurement shows that the material in this region has a high resistivity.

The above results show that as the CdTe growth continues, the amount of excess Te in the melt increases due to the segregation of Cd; and more Te is incorporated into the crystal in the form of V_{Cd}. As a result, during the post-growth cooling period, more complexes and Te precipitates are formed toward the top of the crystal to compensate for the Te_{Cd} and to reduce the infrared transmission.

Since the undoped CdTe are n-type,[2] arsenic, which are acceptors in CdTe, were introduced into the growth melt for producing high resistivity crystals. With an arsenic dose of 2×10^{17} cm^{-3}, CdTe with a resistivity of 1.5×10^{10} Ω·cm were produced. The transmission curves measured on the high resitivity material do not exhibit the fall off found in Curves 1 and 2 in Figure 2. The [241]Am and [57]Co spectra measured by detectors fabricated on the high resistivity CdTe are shown in Figure 3(a) and 3(b), respectively. The radiation peaks in [241]Am can be observed, but the resolution is low. On the other hand, the [57]Co peaks are not present. It is evident that the hole and/or electron trapping is rather severe in the CdTe crystal.

$Cd_{0.9}Zn_{0.1}Te$ Material and Detector

The infrared transmission curves measured on $Cd_{0.9}Zn_{0.1}Te$ are shown in Figure 4. Since the undoped $Cd_{0.9}Zn_{0.1}Te$ crystals are p-type, the free electron absorption shown in Curves 1 and 2 in Figure 2 are not found in the 10% Zn CZT. In reality, both undoped and indium-doped have similar transmission curves. Curve 1 in Figure 4 represents the transmission measured from a $Cd_{0.9}Zn_{0.1}Te$ section 0% to 50% from the bottom of the boule. The high transmission from 2.2 – 22.0μm indicates few Te precipitates in this wavelength range. Curve 2 in Figure 4 is the typical transmission curve measured from a section 50% to 85% from the bottom of the crystal. Slight transmission reduction is observed below 3.3μm, indicating the existence of Te precipitates with sizes smaller than the magnitude of this wavelength. The transmission measured from the top 15% of the $Cd_{0.9}Zn_{0.1}Te$ crystal is shown in Figure 4(a). The reduction in the transmission up to 20.0μm indicates the existence of Te precipitates with all sizes up to this dimension.

The near transmission curves measured on wafers sliced from various sections of the $Cd_{0.9}Zn_{0.1}Te$ are shown in Figure 5. From the bottom to the top of the crystal, the transmission decreases monotonically, demonstrating the increasing amount of the density of small Te-precipitates.

A low indium doping of 2.5×10^{15} cm^{-3} is sufficient to compensate for the residual V_{Cd} over Te_{Cd} in $Cd_{0.9}Zn_{0.1}Te$ for the crystal to reach a high resisvity of 2×10^{10} Ω·cm. The [241]Am and [57]Co spectra measured by detectors fabricated on the high resistivity $Cd_{0.9}Zn_{0.1}Te$ are shown in Figure 6(a) and 6(b), respectively. Both exhibit excellent resolutions of the radiation peaks. The FWHM of the [57]Co 122keV peak is 5.3%.

$Cd_{0.85}Zn_{0.15}Te$ Material and Detector

Figure 7 shows the transmission curve measured on a section, 20% to 50% from the bottom of a typical high resitivity, indium-doped $Cd_{0.85}Zn_{0.15}Te$ crystal. Comparing this curve to those measured on CdTe and $Cd_{0.9}Zn_{0.1}Te$ in similar boule sections, the infrared transmission of $Cd_{0.85}Zn_{0.15}Te$ in the 2.2-13μm range is clearly lower. This result leads to the conclusion that under identical growth conditions, more Te precipitates exists in $Cd_{0.85}Zn_{0.15}Te$ than CdTe and $Cd_{0.9}Zn_{0.1}Te$.

An indium doping of 3.0×10^{15} cm^{-3} was introduced to compensate for the residual V_{Cd} over Te_{Cd} in $Cd_{0.9}Zn_{0.1}Te$ for the crystal to reach a high resisvity of 1.2×10^{10} Ω·cm. The [241]Am and [57]Co spectra measured by detectors fabricated on the high resistivity $Cd_{0.85}Zn_{0.15}Te$ are shown in Figure 8(a) and 8(b), respectively. Compared to the spectra in Figure 6 for $Cd_{0.9}Zn_{0.1}Te$, the [241]Am spectrum of $Cd_{0.85}Zn_{0.15}Te$ is very similar. Furthermore, the FWHM of [57]Co 122 keV has a slightly higher value of 5.9%. The major difference is that the $Cd_{0.85}Zn_{0.15}Te$ [57]Co

has a higher noise between the 14keV and the 122keV peaks due to the trapping, clearly related to the higher density of Te-precipitates.

Cd_0.8Zn_0.2Te Material and Detector

The transmission curve in Figure 9 was measured on a section 20% to 50% from the bottom of a typical high resitivity, indium-doped $Cd_{0.8}Zn_{0.2}Te$ crystal. The infrared transmission is substantially lower than those measured on the three crystals discussed early. This result clearly demonstrates that $Cd_{0.8}Zn_{0.2}Te$ has a much higher density of Te-precipitates than CdTe, $Cd_{0.9}Zn_{0.1}Te$, and $Cd_{0.85}Zn_{0.15}Te$. For achieving high resistivity, an indium doping level of $1.3x10^{16}$ cm^{-3} is required. The $Cd_{0.8}Zn_{0.2}Te$ detector's [241]Am and [57]Co spectra shown in Figure 10 are also inferior to those measured by the other three crystals.

4.0 DEFECT MODEL AND DISCUSSIONS

Defect Model

The above results are summarized in Table 1 for analysis. From these data, the following phenomena are observed:

i) As Zn content increases, the infrared transmission measured on the CZT wafers at a given wavelength decrease accordingly, indicating a higher density of Te-precipitates.

ii) As Zn content increases, the infrared transmission measured on the CZT wafers have lower transmissions at longer wavelengths, suggesting the existence of larger Te-precipitates.

iii) As Zn content increases, a higher donor impurity is required for achieving high resistivity, demonstrating increasing amount of uncompensated acceptors.

iv) Among the grown crystal, the best detectors are produced in CZT with 10% Zn. Inferior detectors are produced in CdTe and CZT with a Zn composition equal to or higher than 15%.

v) High [57]Co noises are observed on CdTe, $Cd_{0.85}Zn_{0.15}Te$, and $Cd_{0.8}Zn_{0.2}Te$ detectors at energies below 122keV compared to $Cd_{0.9}Zn_{0.1}Te$ detectors. As Zn content increases from 15% to 20%, this phenomenon is even more pronounced. A hump is actually found in the $Cd_{0.8}Zn_{0.2}Te$ [57]Co spectrum.

A semi-quantitative model depicted in Figure 11 was developed to explain the above observations. The vertical axis is the density of defects and the x-axis is the Zn content in the CZT crystals. As shown, the densities of V_{Cd} and Te_{Cd} in CdTe is on the order of $1x10^{20}$ cm^{-3} at the growth temperature as described in Section 2. As increasing amount of Zn is introduced into CdTe, the density of V_{Cd} increases and that of Te_{Cd} decreases because of the reduction in the lattice parameter. This proposition is consistent with the fact that undoped CZT is n-type without Zn and is p-type with 10% Zn. This is also in agreement with the fact that the undoped ZnTe is always p-type. This proposition is also confirmed by a recent paper.[8] Therefore, the semi-quantitative densities of V_{Cd} and Te_{Cd} are plotted in Figure 11 with V_{Cd} and Te_{Cd} increases and decreases, respectively, with the Zn content.

The difference of the densities of V_{Cd} and Te_{Cd} (V_{Cd}-Te_{Cd}) at room temperature is equivalent to the electron density or the hole density of the undoped CZT crystal and is plotted at the lower portion of Figure 11. Another critical curve is that of the density of the Te-precipitates. Theoretically, Zn atom moves faster than Cd because of their size. Since the diffusion rate of V_{Cd} is proportional to the diffusion rate of Zn and Cd, it can be concluded that V_{Cd} is much more mobile in CZT with a higher Zn content. It is the fast V_{Cd} diffusion rate in high Zn content CZT propels the mergeing of V_{Cd}. This creates a higher density of Te precipitate, which results in a lower transmission in CZT as Zn content increases. Therefore, the curve of Te-precipitates is monotonically increasing with the Zn content in the CZT crystals.

Since in CdTe and CZT with smaller amount of Zn, only small amount of Te-precipitates are formed during the post-growth cooling period by the merges of V_{Cd}, most of the defects generated at the growth temperature will remain either as point defects or form defect complexes such as $Te_{Cd}·V_{Cd}$ and $Te_{Cd}·(V_{Cd})^2$. Therefore, we can expect that the densities of Te_{Cd}, V_{Cd}, and defect complexes all decrease monotonically as CZT Zn content increases.

To construct the curve of Te_{Cd} density, we can assign a density of $1x10^{16}$ cm^{-3} to Te_{Cd} in CZT with 10% Zn as discussed in References 6 and 10. Then, the densities of Te_{Cd} in other crystals can be approximated by the

conclusion of the above discussion. Another factor to support this concept is the Te_{Cd} density at growth temperature in Figure 11, showing a monotonically decreasing Te_{Cd} density as Zn content increases. Hence, we can expect the same trend for the room temperature Te_{Cd} density. The density of V_{Cd} in CZT is simply the sum of the densities of Te_{Cd} and the measured room temperature hole/electron concentration.

Why Zinc?

With the above discussion, the two questions raised in Section 1.0 can be successfully explained. First of all, CdTe and CZT with lower amount of Zn contents have higher density of Te_{Cd} during the growth than CZTs with more Zn content. Although additional V_{Cd} are introduced as the Zn content increases, the density of V_{Cd} can be reduced during the post-growth cooling process because of its fast diffusion rate. As a result, at room temperature, CdTe and low Zn content CZT have many more point defects and defect complexes to trap both electrons and holes. Consequently, the [57]Co 122keV peak cannot even be observed in Figure 3. Therefore, the role of Zn is to reduce the densities of these carrier traps.

How Much?

However, as the Zn content increases to a certain level, the density of V_{Cd} will reach a high level to the degree that during the post-growth cooling, V_{Cd} merge together to form Te-precipitates form before they can diffuse out of the crystals. As a result, the Te-precipitates trap the carriers and degrade the detector resolution. The 60keV hump in Figure 10(b) can be assigned to this effect.

Based on our results, the CdTe and $Cd_{0.9}Zn_{0.1}Te$ have poor detector resolution because of the trapping of charge carrier by Te_{Cd}, V_{Cd}, and complexes such as $Te_{Cd} \cdot V_{Cd}$ and $Te_{Cd} \cdot (V_{Cd})$. $Cd_{0.8}Zn_{0.2}Te$ has a serious trapping of charge carriers by Te-precipitates. The high noise of $Cd_{0.85}Zn_{0.15}Te$ below 122keV in Figure 8(b) even shows some Te-precipitates trapping effects. Therefore, CZT with content near 10% offers the best detectors.

It should be noted though that the above discussion is limited to crystals grown under our specific conditions. Crystals grown differently may draw slightly different conclusions as to the optimal Zn content for producing the best detectors. The purpose of this paper is to present the mechanism of how defect evolvement affects the crystal material and detector and new growth approaches can be developed to optimize the CZT detector performance.

5.0 SUMMARY

CZT. crystals with Zn contents of 0%, 10%,15%, and 20% have been grown and detectors have been produced. Infrared transmission measured on the wafers sliced from these crystals shows that as the Zn content increases, there is a reduction in the transmission toward longer wavelength, indicating the existence of an increasing amount of larger Te-precipitate. For producing high resistivity materials, a higher concentration of indium is also required for CZT with higher Zn content. The best detectors were produced in CZT with 10% Zn, while CdTe detectors was not able to resolve the [57]Co 122keV peak. In addition, CZT detectors with 15% and 20% Zn display high noise level at energies below this peak.

These results are explained by a model that the role of Zn in CZT is to reduce the density of Te_{Cd}, to increase the density of V_{Cd}, and to enhance the diffusion rate of V_{Cd}. The higher amounts of Te-precipitates in CZT with more Zn is caused by the rapid merge of V_{Cd} through fast diffusion of V_{Cd}. Because of the trapping by Te-precipitates, detectors fabricated on CZT with 10% and 20% Zn are inferior to the 10% Zn CZT detectors. On the other hand, CdTe and CZT with Zn content less than 7% Zn have a high concentration of Te_{Cd}, V_{Cd}, and complexes such as $Te_{Cd} \cdot V_{Cd}$ and $Te_{Cd} \cdot (V_{Cd})$, which are also trapping centers. As a result, the detectors fabricated on these crystals are also inferior to the 10% Zn detectors. The optimal Zn content for CZT grown using our technique is therefore near 10%.

REFERENCES

1. Csaba Szeles, The 2002 U.S. Workshop on the Physics and Chemistry of II-VI Materials, San Diego.

2. M. Chu, S. Terterian, D. Ting, S. Mesropian, R.H. Gurgenian, and C.C. Wang, Appl. Phys. Lett. 79, 2728 (2001).
3. R. Grill, J. Franc, P.Hoschl, I. Turkevych, E. Belas, P. Moravec, M. Fiederle, and K.W. Benz, IEEE Transaction on Nuclear Science, 49, 1250, 2002.
4. A. Zumbiehl, M. Hage-Ali, M.Ayoub, R. Regal, J.M. Koebel, and P. Siffert, IEEE Transaction on Nuclear Science, 49, 1254, 2002
5. M. Chu, S. Terterian, D. Ting, R.B. James, M. Szawlowski, and G.J. Visser, SPIE Proceedings, Vol. 4784A, 237, Seattle, 2002.
6. M. Chu, S. Terterian, D. Ting, C.C. Wang, J.D. Benson, J.H. Dinan, R.B. James, and A. Burger, J. of Electron Mater. 32, 778 (2003).
7. S. Terterian, M. Chu, D. Ting, C.C. Wang, M. Szawlowski, G.J. Visser, and Paul Luke, J. of Electron Mater, 32, 796 (2003).
8. J.H. Greenberg, The 2003 U.S. Workshop on the Physics and Chemistry of II-VI Materials, New Orleans, Submitted to J. Electron. Mater.

9. S. Terteerian, M. Chu, and D. Ting, The 2003 U.S. Workshop on the Physics and Chemistry of II-VI Materials, New Orleans. Submitted to J. Electron. Mater.

10. M. Fiederle, C. Eiche, M. Salk, R. Schwarz, K.W. Bens, W. Stadler, D.M. Hofmann, and B.K. Meyer, J. Appl. Phys, 84, 6689 (1998).
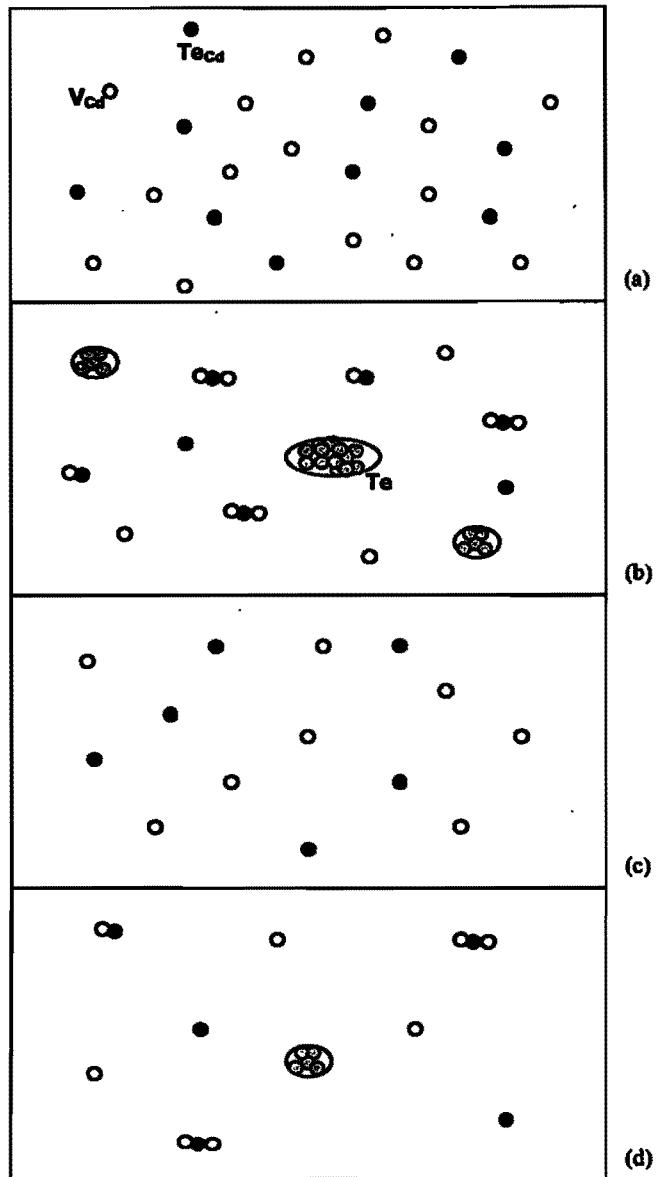
Fig. 1 Evolvements of V_{Cd} and Te_{Cd} generated at growth temperature into defect complexes and Te precipitates during the post growth cooling period.
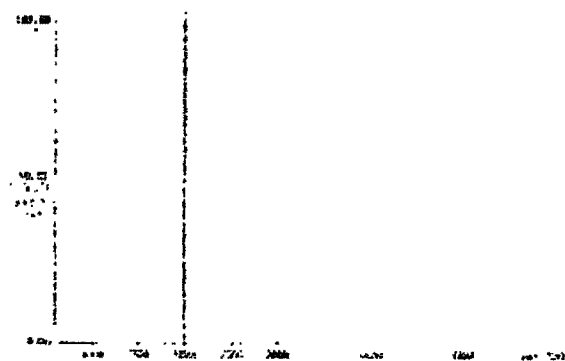
Curve 4
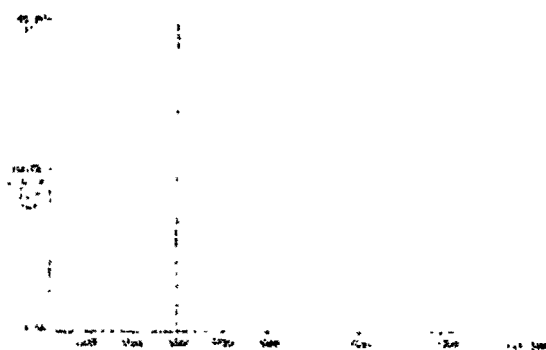
Curve 3
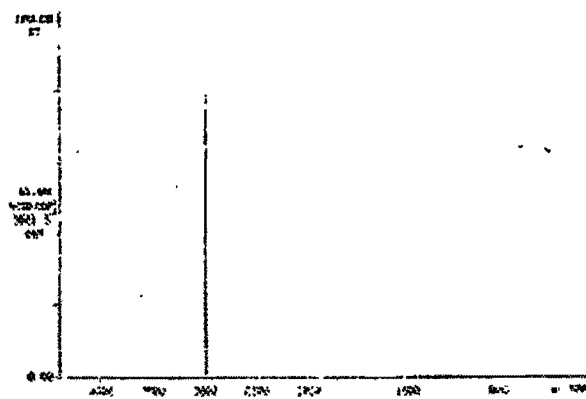
Curve 2
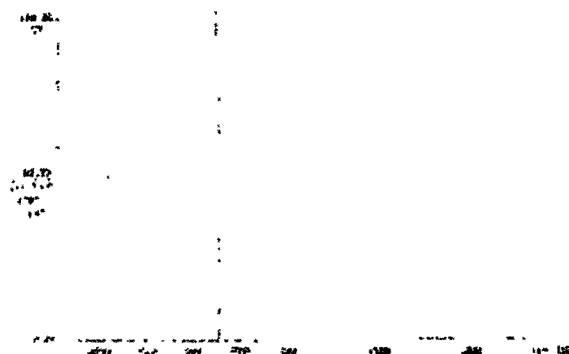
Curve 1

Fig. 2 Infrared transmission curves measured at various sections of CdTe. Sequentially, curves 1 to 4 were measured from the bottom to the top of the crystal.
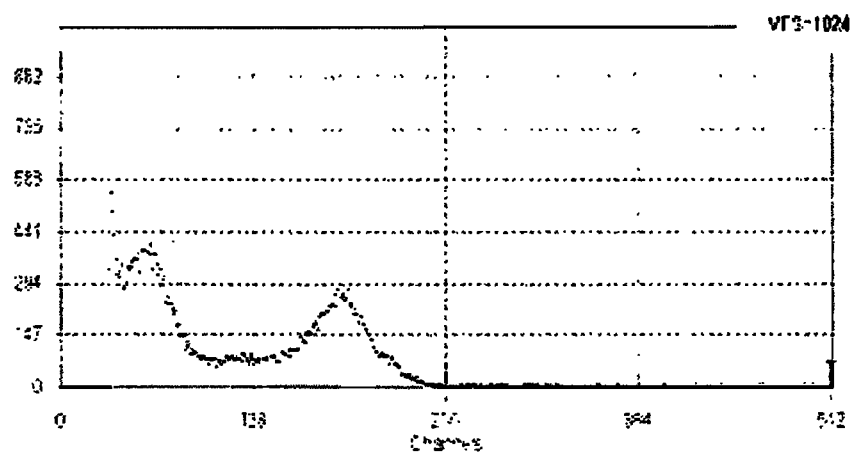
(a)
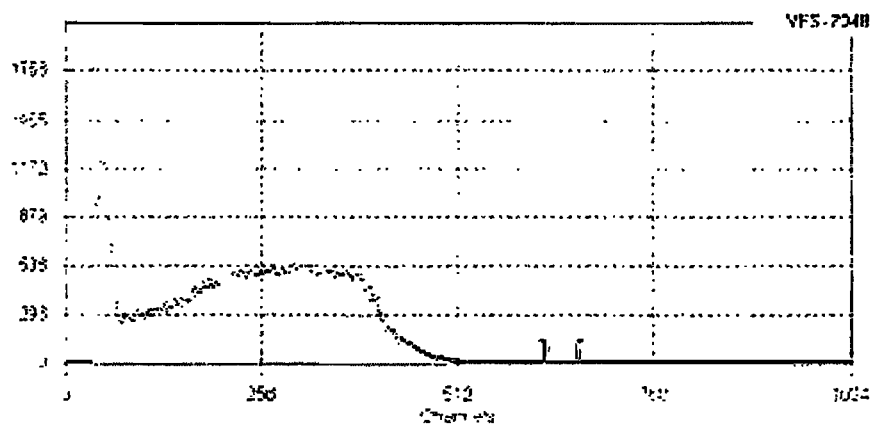
(b)

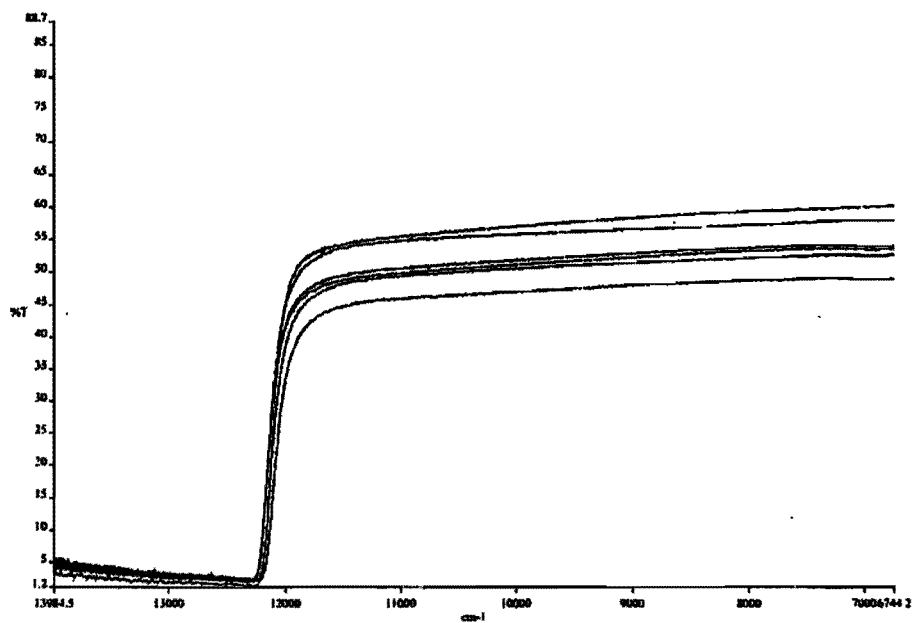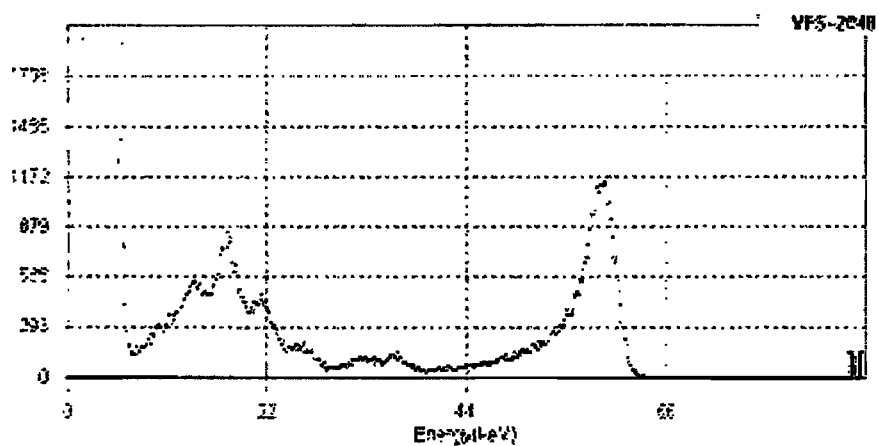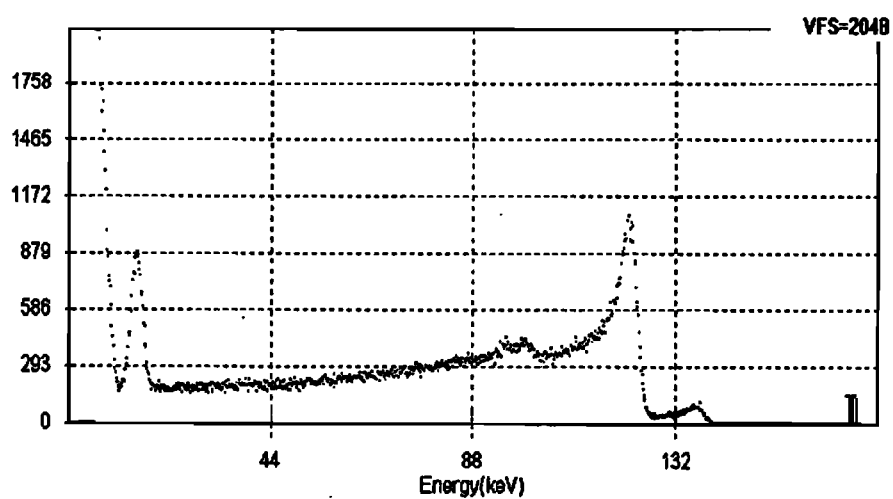Fig. 3 (a) ^{241}Am and (b) ^{57}Co spectra measured by CdTe detector.
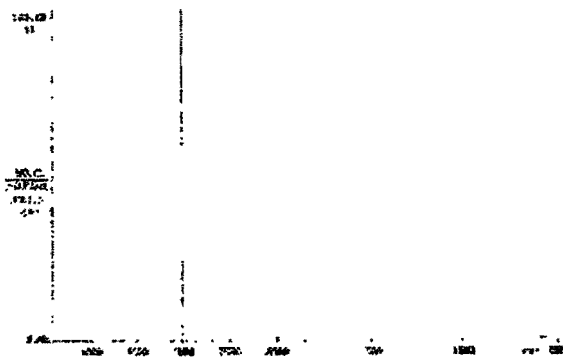
Curve 3
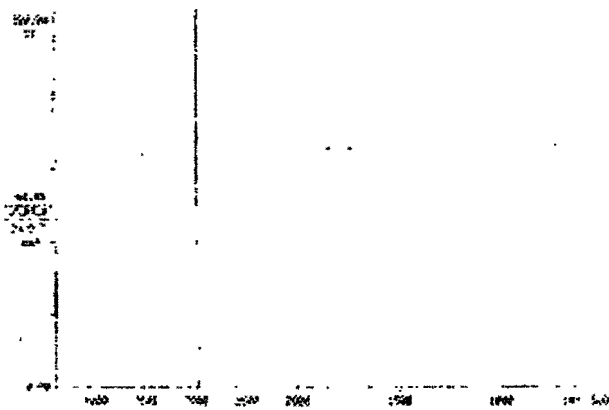
Curve 2
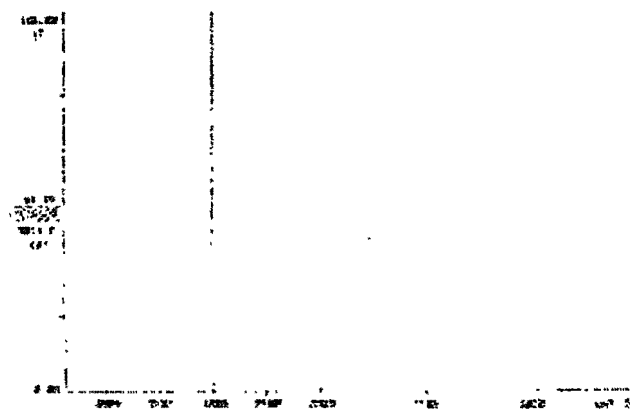
Curve 1

Fig. 4 Infrared transmission curves measured at various sections of $Cd_{0.9}Zn_{0.1}Te$. Sequentially, Curves 1 to 3 were measured from the bottom to the top of the crystal.

Fig. 5 Near infrared transmission curves measured at various sections of $Cd_{0.9}Zn_{0.1}Te$. From the bottom to the top portion of the crystal, the transmission deceases sequentially.

(a)

(b)

Fig. 6 (a) ^{241}Am and (b) ^{57}Co spectra measured by $Cd_{0.9}Zn_{0.1}Te$ detector.
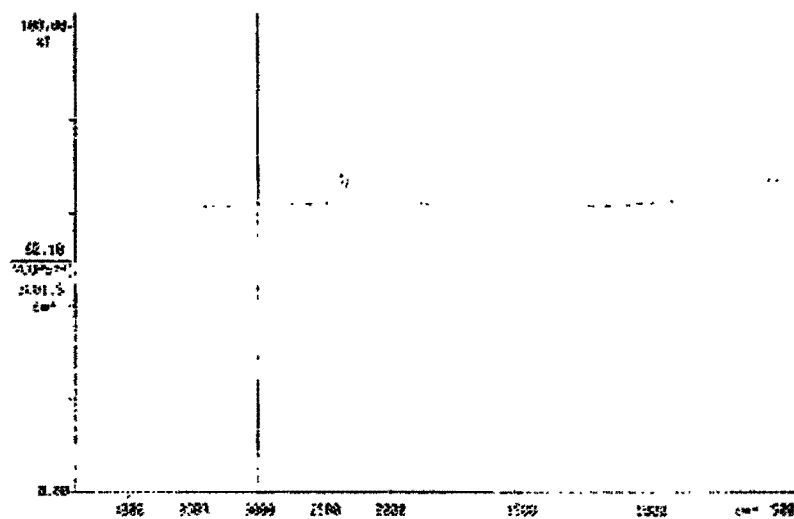
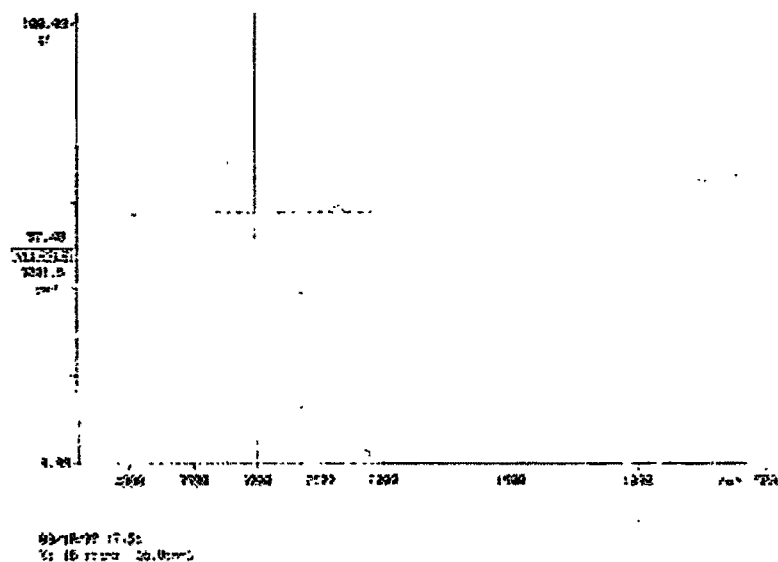Fig. 7 Infrared transmission curve measured at the section 20 – 50% from the bottom of $Cd_{0.85}Zn_{0.15}Te$.
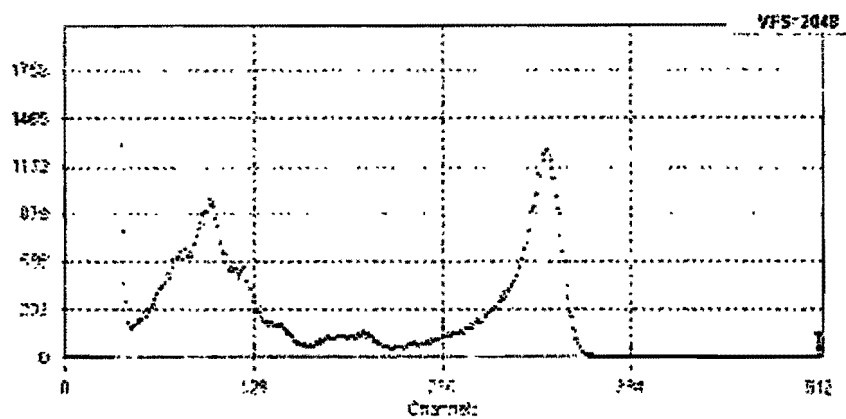
(a)
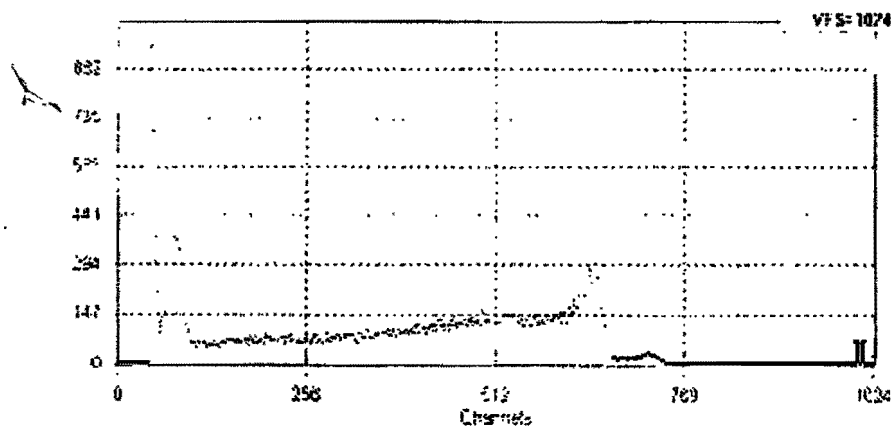
(b)

Fig.8 (a) ^{241}Am and (b) ^{57}Co spectra measured by $Cd_{0.85}Zn_{0.15}Te$ detector.

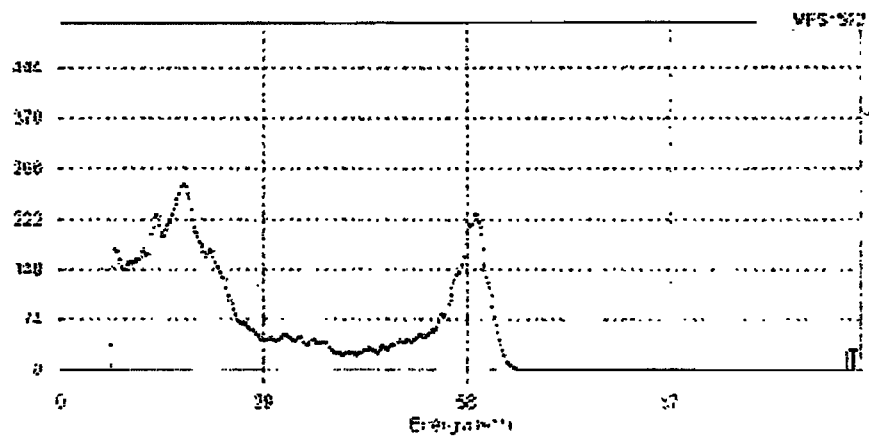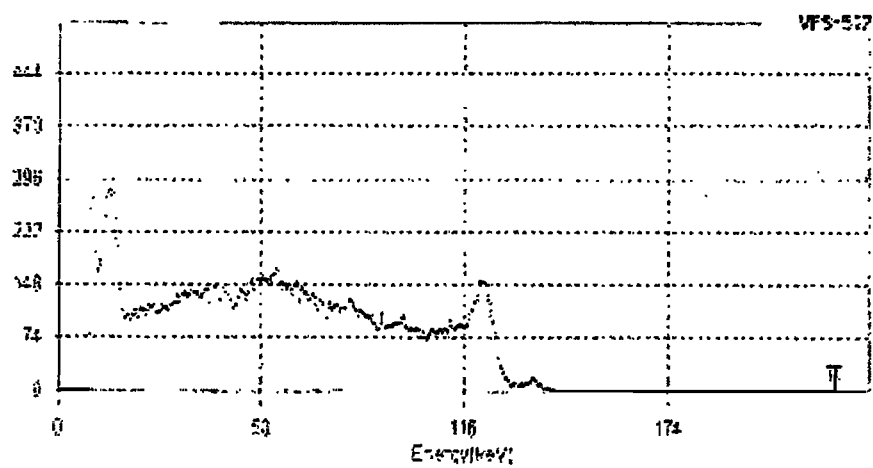Fig. 9 Infrared transmission curve measured at the section 20 – 50% from the bottom of $Cd_{0.8}Zn_{0.2}Te$.

(a)

(b)

Fig. 10 Fig.8 (a) ^{241}Am and (b) ^{57}Co spectra measured by $Cd_{0.8}Zn_{0.2}Te$ detector.
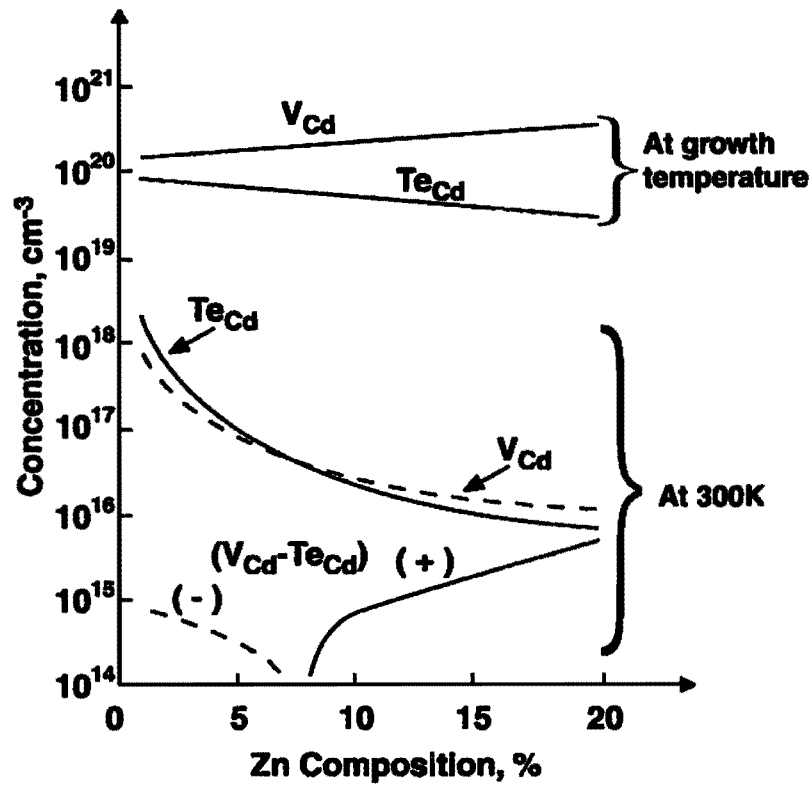
Fig. 11 Qualitative defect model showing densities of defects at growth temperature and room temperature. At room temperature, the density of Te precipitates increases with the Zn content while defect complexes such as $Te_{Cd} \cdot V_{Cd}$ and $Te_{Cd} \cdot (V_{Cd})^2$ decease as Zn content increases.

Table 1 Summary of material and detector characteristics of CZT with different amount of Zn.

Zn Content	Transmission @		Dopant	Dose (cm^{-3})	Resistivity ($\Omega \cdot$cm)	^{57}Co 122keV FWHM	Noise Below ^{57}Co 122keV
	3.3μm	10μm					
0%	65.1	65.5	Arsenic	2x10^{17}	1.5x10^{10}	No Peak	High
10%	64.5	65.0	Indium	2.5x10^{15}	2.0x10^{10}	5.3%	Low
15%	62.1	62.5	Indium	3.0x10^{15}	1.2x10^{10}	5.9%	Medium
20%	57.5	60.5	Indium	1.3x10^{16}	1.1x10^{10}	15%	Hump

DEPARTMENT OF DEFENSE

DEFENSE TECHNICAL
INFORMATION CENTER
8725 JOHN J. KINGMAN ROAD,
SUITE 0944
FT. BELVOIR, VA 22060-6201
        ATTN: DTIC/OCA

DEPARTMENT OF DEFENSE
CONTRACTORS

EXELIS, INC.
1680 TEXAS STREET, SE
KIRTLAND AFB, NM 87117-5669
        ATTN: DTRIAC